Bioorg. Med. Chem. 31 (2021) 115969

Contents lists available at ScienceDirect

Bioorganic & Medicinal Chemistry

journal homepage: www.elsevier.com/locate/bmc

Design, synthesis and anti-inflammatory activity of imidazol-5-yl pyridine derivatives as p38α/MAPK14 inhibitor

Eslam M.H. Ali [a,b,c], Mohammed S. Abdel-Maksoud [d], Rasha Mohamed Hassan [d], Karim I. Mersal [a,b], Usama M. Ammar [e], Choi Se-In [f], Han He-Soo [f], Hee-Kwon Kim [g,h], Anna Lee [i], Kyung-Tae Lee [f,*], Chang-Hyun Oh [a,b,*]

[a] Center for Biomaterials, Korea Institute of Science & Technology (KIST School), Seoul, Seongbuk-gu, 02792, Republic of Korea
[b] University of Science & Technology (UST), Daejeon, Yuseong-gu, 34113, Republic of Korea
[c] Pharmaceutical Chemistry Department, Faculty of Pharmacy, Modern University for Technology and Information (MTI), Cairo 12055, Egypt
[d] Medicinal & Pharmaceutical Chemistry Department, Pharmaceutical and Drug Industries Research Division, National Research Centre (NRC), (ID: 60014618), P.O. 12622, Dokki, Giza, Egypt
[e] Strathclyde Institute of Pharmacy and Biomedical Sciences, University of Strathclyde, 161 Cathedral Street, Glasgow G4 0NR, Scotland, United Kingdom
[f] Department of Pharmaceutical Biochemistry, College of Pharmacy, Kyung Hee University, 1 Hoegi-dong, Dongdaemun-gu, Seoul 130-701, Republic of Korea
[g] Department of Nuclear Medicine, Molecular Imaging & Therapeutic Medicine Research Center, Jeonbuk National University Medical School and Hospital, 20 Geonji-ro, Deokjin-gu, Jeonju 54907, Republic of Korea
[h] Research Institute of Clinical Medicine of Jeonbuk National University-Biomedical Research Institute of Jeonbuk National University Hospital, 20 Geonji-ro, Deokjin-gu, Jeonju 54907, Republic of Korea
[i] Department of Chemistry, Hanseo University, Seosan 31962, Republic of Korea

ARTICLE INFO

Keywords:
P38α
Anti- inflammatory
Pharmacophore
TNF-α
1L-6
1L-1β Nitric Oxide
PGE2

ABSTRACT

P38α/MAPK14 is intracellular signalling regulator involved in biosynthesis of inflammatory mediator cytokines (TNF-α, IL-1, IL-6, and IL-1b), which induce the production of inflammatory proteins (iNOS, NF-kB, and COX-2). In this study, drug repurposing strategies were followed to repositioning of a series of B-RAF ^{V600E} imidazol-5-yl pyridine inhibitors to inhibit P38α kinase. A group 25 reported P38α kinase inhibitors were used to build a pharmacophore model for mapping the target compounds and proving their affinity for binding in P38α active site. Target compounds were evaluated for their potency against P38α kinase, compounds **11a** and **11d** were the most potent inhibitors (IC_{50} = 47 nM and 45 nM, respectively).

In addition, compound **11d** effectively inhibited the production of proinflammatory cytokines TNF-α, 1L-6, and 1L-1β in LPS-induced RAW 264.7 macrophages with IC_{50} values of 78.03 nM, 17.6 μM and 82.15 nM, respectively.

The target compounds were tested for their anti-inflammatory activity by detecting the reduction of Nitric oxide (NO) and prostaglandin (PGE2) production in LPS-stimulated RAW 264.7 macrophages. Compound **11d** exhibited satisfied inhibitory activity of the production of PGE2 and NO with IC_{50} values of 0.29 μM and 0.61 μM, respectively. Molecular dynamics simulations of the most potent inhibitor **11d** were carried out to illustrate its conformational stability in the binding site of P38α kinase.

1. Introduction

Mitogen-activated protein kinases (MAPKs) are crucial signalling components that become activated in response to extracellular stimuli such as growth factors and regulate a wide range of cellular processes such as proliferation, stress responses, apoptosis and immune defence.[1,2] Deregulations of MAP kinases expression are associated with numerous diseases including neurodegenerative impairment such as Alzheimer's disease, autoimmune diseases such as rheumatoid arthritis (RA), inflammatory disorders, and sometimes cancer.[3–6] P38 MAPK pathway is one of the major MAPK pathways, which is also called stress-activated protein kinase pathway as it is activated by environmental stress such

* Corresponding authors at: Center for Biomaterials, Korea Institute of Science & Technology (KIST School), Seoul, Seongbuk-gu, 02792, Republic of Korea (C.-H. Oh).
E-mail addresses: ktlee@khu.ac.kr (K.-T. Lee), choh@kist.re.kr (C.-H. Oh).

https://doi.org/10.1016/j.bmc.2020.115969
Received 25 October 2020; Received in revised form 20 December 2020; Accepted 21 December 2020
Available online 28 December 2020
0968-0896/© 2020 Elsevier Ltd. All rights reserved.

as UV radiation, osmotic shock, and mechanic stress) and genotoxic stresses.[7] P38 MAPKs have four isoforms: p38α (MAPK14), p38β (MAPK11), p38γ (MAPK12), and p38δ (MAPK13).[8] P38α (MAPK14) is highest expressed isoform in most cell types and so p38α is the most frequent drug target reported in the published literature[9,10].

Chronic inflammation progression is compelled by incessant activation of inflammatory mediators cytokines like tumor necrosis factor-a (TNF-α), interleukin-1 (IL-1), interleukin-6 (IL-6), and interleukin-1b (IL-1β), whose biosynthesis and release is regulated by the activity of p38α kinase.[11–13] Activation of TNF- α and IL-1β induces the production of other inflammatory proteins such as inducible nitric oxide synthase (iNOS), prostaglandins (PGs), receptor activator of nuclear factor NF-kB ligand (RANKL), and cyclooxygenase 2 (COX-2).[14] In addition to its role in production of proinflammatory cytokines, p38α kinase regulates cytosolic phospholipase phosphorylation and promotes its synthesis at transcriptional and translational level.[15] Therefore, p38α kinase activation state is linked to stimulation-induced PGE2/NO production.

Several small molecules have been reported in the literature as p38α kinase inhibitors[16–29] (Fig. 1).

In a previous work, we reported a series of imidazol-5-yl pyridine derivatives as potential B-RAF^{V600E} inhibitors.[30] Both p38α kinase and B-RAF kinase are key components in MAPK pathway; B-RAF kinase binds with RAS as the upstream activator, and mediate the MAPK signaling transduction to the MEK resulted to the activation of downstream MEK1/2 and ERK1/2 which is the upstream regulator of stress-activated protein kinase MsK1/2,[31] whereas, p38α kinase is activated by the upstream MKK3/6, and sometimes by MKK4, p38α kinase regulates protein kinases, including MAPK-activated kinase 2 MK2, mitogen- and stress-activated protein kinase 1 MsK1, and MAP kinase-interacting serine/threonine MNK1/2.[9,32,33] In the current work, the synthesized compounds were evaluated for its P38α inhibitory activity, compound **11d** was the most potent inhibitor with IC_{50} value of 45 nM.

Further anti-inflammatory assays were conducted to the target compounds, compound **11d** exhibited satisfied inhibitory activity of the production of PGE2 and NO with IC_{50} values of 3.8 μM and 8.4 μM, respectively. Also, compound **11d** effectively inhibited the production

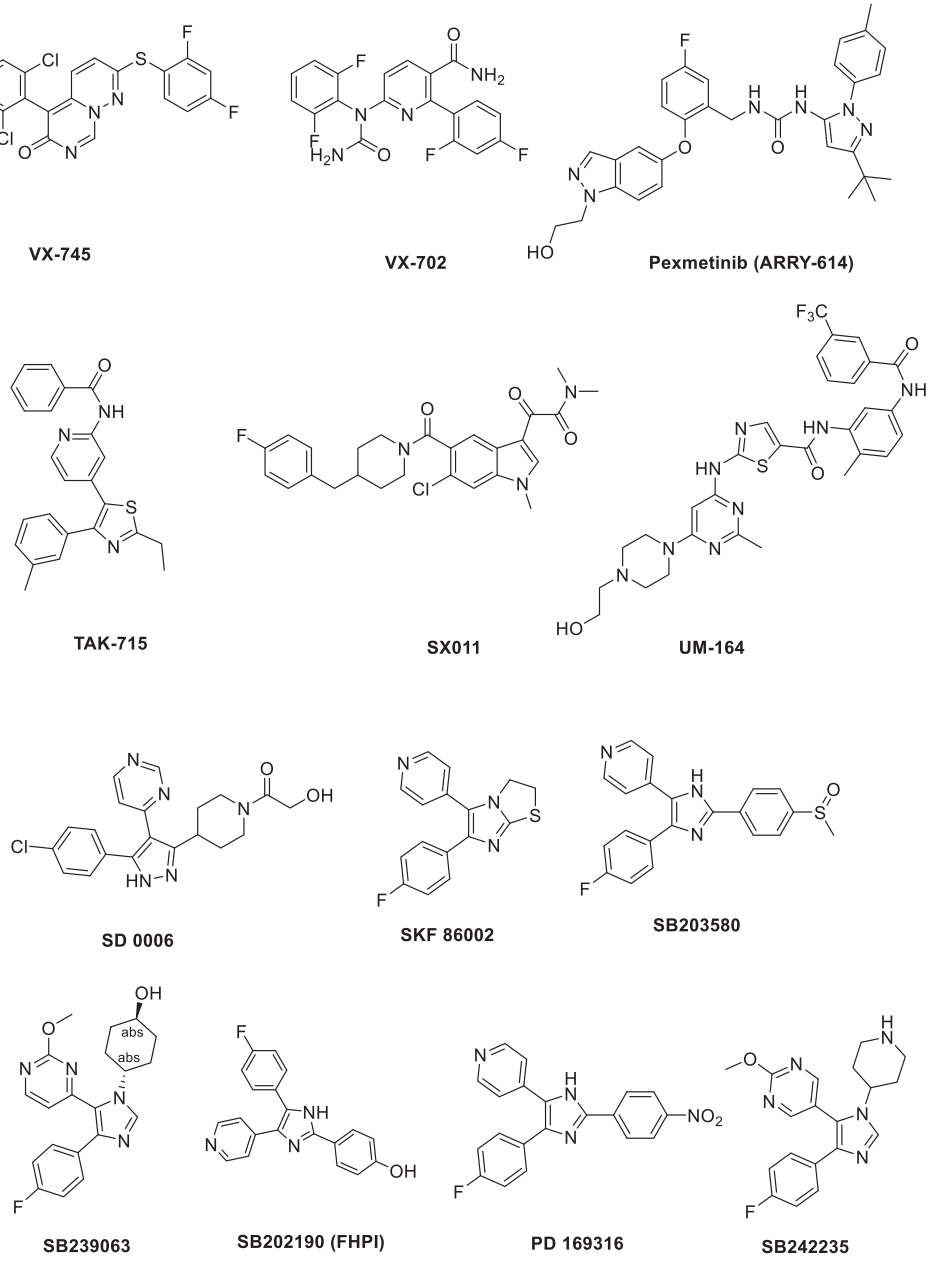

Fig. 1. Structures of 25 reported P38α/MAPK14 inhibitors (pharmacophore training set).

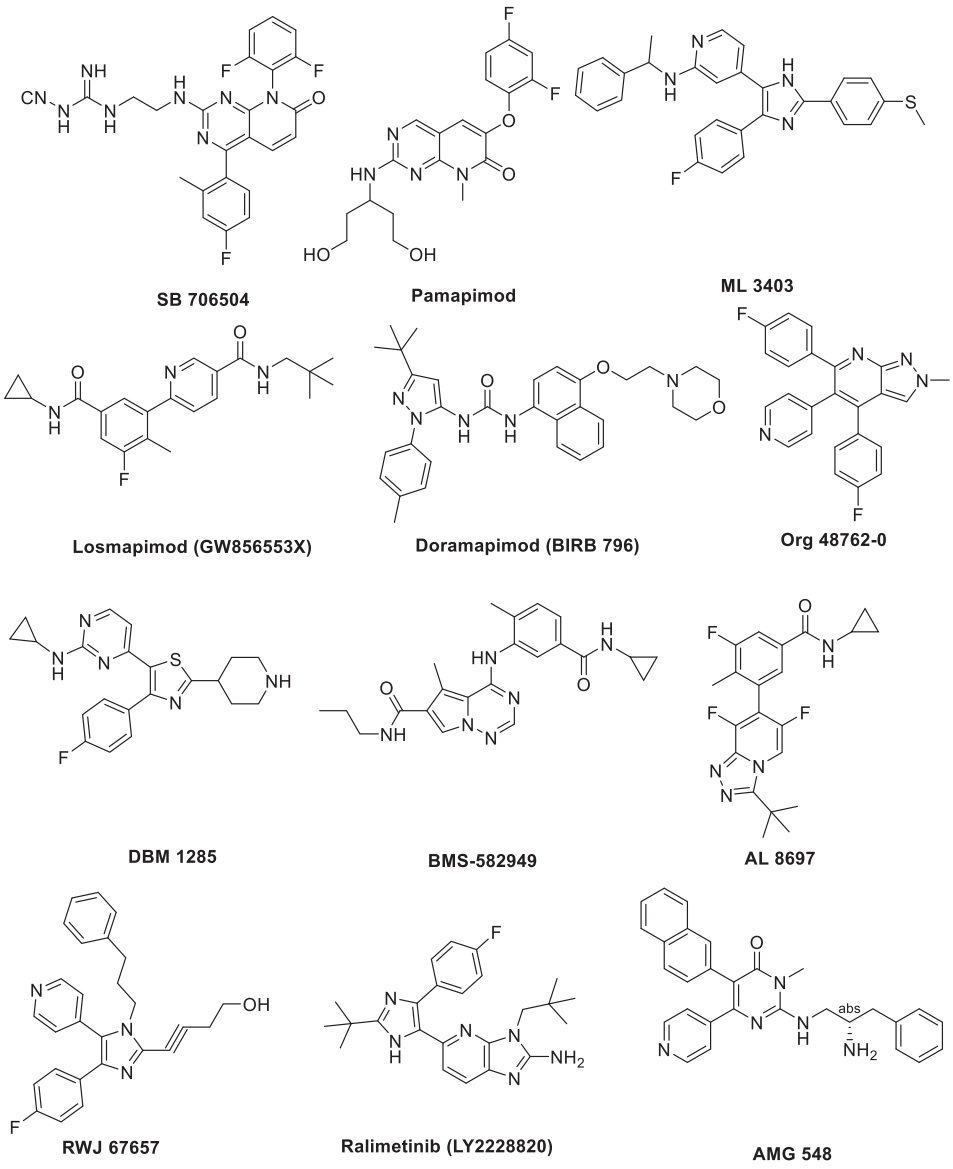

Fig. 1. (*continued*).

of TNF-α, 1L-6, and 1L-1β inflammatory cytokines in LPS-induced RAW 264.7 macrophages with IC_{50} values of 78.03 nM, 17.6 μM and 82.15 nM, respectively.

Molecular modelling studies included molecular docking for the target compounds, and molecular dynamics simulation for the most active hit **11d** were conducted in attempt to emphasis the relation between the mentioned kinase inhibitory activity for each derivative and their molecular interaction and stability in the active site of P38α kinase.

2. Results and discussion

2.1. Rational and design

In the current work, off-target based drug repurposing strategies were followed in order to reposition B-RAF targeted inhibitors to inhibit p38α kinase.

2.1.1. Protein alignment

In this study, Molecular Operating Environment (MOE, 2014) software was used to operate ligand binding site alignment protocol of the two corresponding protein kinases p38α (PDB: 3GCP) and B-RAF (PDB: 4XV2).

The two crystal structures were downloaded from PDB, their energies were minimized, and were subjected to flexible alignment, where the initial pairwise similarity matrix was build first using either a progressive or a tree-based method. Then a round-robin realignment is performed, followed by a randomized iterative refinement. The structure based realignment is performed using the existing secondary element information. After this, 3D superposition has been done on the best aligned model.[34]

This direct comparison of the two enzymes binding sites describes the ligand molecular binding to provide useful insights into the compound molecular interaction mode. The result of the two pockets superposition approved the alignment of the essential interacted amino acids in the two kinases active site. As illustrated in Fig. 2, the two enzymes superposition showed high alignment in the adenine hinge area, ribose pocket, and hydrophobic back pocket. The two native ligands (**Dabrafenib** (P06) and **SB203580** (SB2)) of the corresponding kinases bind in the hinge region via interaction with Cys532 and Met109 amino acids, the central 5-membered ring native ligands is buried in the deep ribose pocket through interactions with Val471 and Val38 in BRAF and P38α respectively.

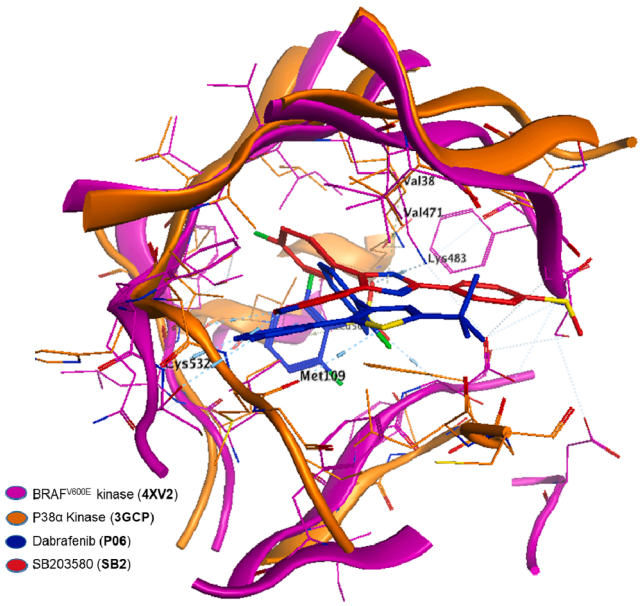

Fig. 2. Superposition of B-RAF^{V600E} kinase (PDB: 4XV2) and p38α kinase (PDB: 3GCP) binding pockets showing the alignment between their ligands **Dabrafenib** (P06) and **SB203580** (SB2).

2.1.2. The SAR of the reported P38α inhibitors

Many studies have reported imidazole-based derivatives acting as a potent p38α kinase inhibitors where **SB203580** the pyridin-4-ylimidazole derivative was used as a lead compound to prepare imidazole-based derivatives act as ATP mimetic for inhibition of p38α kinase as a target in inflammation therapy.[16,35–38] In this regard, the structural modifications of the lead compound **SB203580** led to improving the p38α kinase inhibitory activity, which in turn get insight into the structural activity relationship of the designed inhibitors. Such modifications were illustrated in replacing the central imidazole ring by bicyclic benzopyrazines and pyrazolo pyrimidines or by triazole ring resulted in more potent P38α kinase inhibitors with good anti-inflammatory activity.[39–42] Furthermore, replacement of the pyridinyl moiety in the hinge binding area by hetero bicyclic ring boosted the molecular interactions in P38α kinase binding site through the additional H-bond and afforded new candidates with potent enzyme inhibitory activity.[41,43]

The essential interactions of **SB203580** inhibitor with the ATP-binding cleft are briefly illustrated in (Fig. 3, a), where the 2-aminopyridyl residues bonds to the adenine hinge binding region by hydrogen bond acceptor, while, the para fluoro phenyl moiety occupies the hydrophobic back pocket. The central imidazole ring embeds into the ribose pocket and possesses H-bond interaction with the NH of Lys53. In addition, the phosphate phosphate binding region is occupied with 4-(methylsulfinyl)phenyl at position 2 of the imidazole ring.[1] The structural similarity between our Imidazolyl pyridine series and both **SB203580** and other reported imidazole-based inhibitors brought our attention to predict their binding mode and their biological activity, as well. In this work, Imidazolyl pyridine derivatives were proposed to conserve the molecular interaction behavior of **SB203580** alongside additional interactions to bring the target compounds higher binding affinity. In designing of our compounds we also guided by the reported SAR studies of tri substitution on the central imidazole scaffold, which resulted in the production of pyridinylimidazole derivatives possessing different substitution at C2-pyridine that rendered the produced candidates higher affinity into the enzyme binding site and better inhibitory activity.[44] As a result, in addition to the essential binding mode of **SB203580**, the target derivatives were expected to bind strongly in the hinge adenine region through an additional H-bond between the NH at position 2 of the pyridine and the carbonyl oxygen of Met109, the terminal sulphonamide moiety with ethyl or propyl spacer was to orient the sulphonamide aromatic moiety towards the hydrophobic front pocket (Fig. 3, b).

2.1.3. Pharmacophore model development

Pharmacophore model were developed using MOE software. The 3D pharmacophore model was built using reported p38α kinase which can properly detect SAR of the existing p38α kinase inhibitors. Then, the model was used as 3D search query for predicting the structural requirements of each compound to identify p38α kinase new inhibitors. In this study, a training set of 25 p38α kinase inhibitors with structural diversity and wide range of inhibitory activity were collected from different research papers (Fig. 1). All compounds were built in 2D structure using ChemDraw software, MOE software was used for the molecular 3D visualization and minimization to the closest local minimum using the CHARMm-like force field. The pharmacophore query was generated using hydrogen bond acceptor (HBA), hydrogen bond donor (HBD), hydrophobic (H) and ring aromatic (RA) chemical features. A group fifteen energetically reasonable conformational models were generated. The selected pharmacophore model represented by two hydrophobic centers (F1: Hyd/Aro and F2: Hyd/Aro), one aromatic center (F3: Aro), and one center (F4: ML/Acc/Don) including H-bond donor (Don), the H-bond acceptor (Acc), and metal ligator (ML) (Fig. 4).

The produced pharmacophore model was used for mapping the imidazolyl pyridine target compounds and the RMSD values were determined less than 1. The target compounds showed typical fitting in the pharmacophore model. As shown in Fig. 5, the first hydrophobic centre F1 was represented by the terminal aromatic sulphonamide group, the phenyl moiety at C2 of the imidazole signified the second hydrophobic centre F2, while the lateral pyridine ring represented aromatic centre F3, the nitrogen atom of pyridine represented the H-bond acceptor (Acc) part in (F4: ML/Acc/Don) centre.

2.2. Chemistry

Synthesis of the target compounds **8a-i**, **9a-i**, **10a-j**, and **11a-j** was fulfilled according to Scheme 1. Esterification of the 3-methoxy-4-chlorobenzoic acid **1** to its corresponding methyl ester **2** was carried out by reaction with methanol in the presence of sulphuric acid. In basic media of lithium bis(trimethylsilyl)amide (LiHMDS), the methyl ester **2** reacted with 2-bromo-4-methylpyridine to afford 2-(2-bromopyridin-4-yl)-1-(3-methoxyphenyl)ethan-1-one **3**. Imidazole intermediate **5** was prepared by oxidation of **3** by hydrobromic acid in DMSO into 1-(2-bromopyridin-4-yl)-2-(3-methoxyphenyl)ethane-1,2-dione **4**, followed by cyclisation through the reaction with benzaldehyde in presence of ammonium acetate and acetic acid. Reaction of compound **5** with ethylene diamine or propylene diamine afforded compounds **6** and **7**, respectively. Subsequent reaction of **6** or **7** with different aromatic sulfonyl chlorides produced the final target compounds **8a-i** and **9a-i**. The demethylated derivatives **10a-j** and **11a-j** were obtained by demethylation of **8a-i** or **9a-i** by boron tribromid −70 °C in presence of catalytic amount of tetrabutylammonium iodide under N_2 atmosphere. The key structure of the target compounds is illustrated in Table1.

2.3. Biological evaluation

2.3.1. In vitro p38a kinase inhibitory activity

The synthesized target compounds were evaluated for their *In vitro* p38a kinase inhibitory activity using ELISA technique (enzyme-linked immunosorbent assay). The inhibition activities for each derivative are illustrated in Table 2. The preliminary data revealed that the tested compounds exhibited a wide range of inhibitory activity against p38a/MAPK14 Kinase. Over all, compounds **10a-j** and **11a-j** with 3-hydroxy phenyl moiety at position 4 of the imidazole ring exhibited a slight higher inhibitory activity than the 3-methoxy phenyl containing

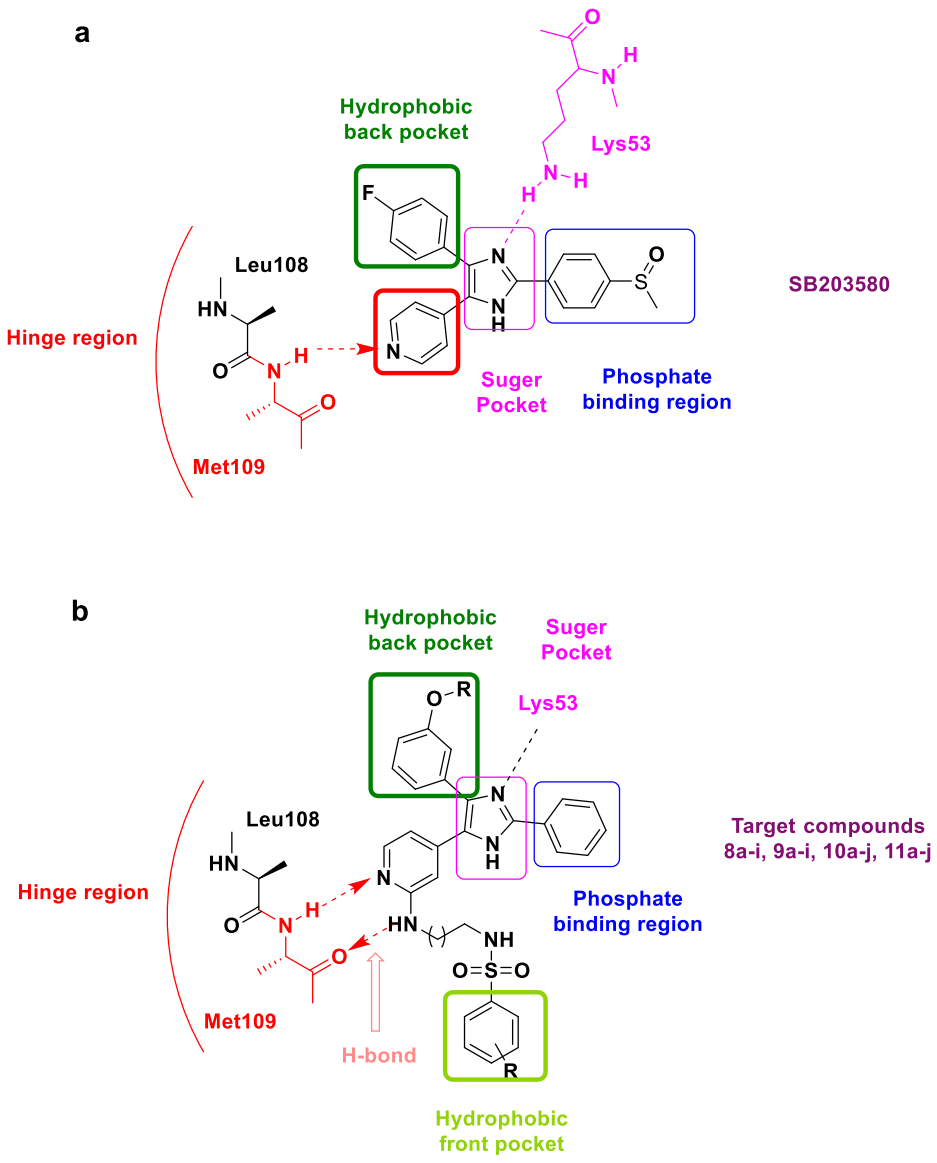

Fig. 3. (a) Binding mode of **SB203580** into ATP binding site (PDB: 3GCP), (b) proposed binding mode of the target inhibitors into the ATP-binding.

derivatives **8a-i** and **9a-i**, in addition, derivatives **9a-i** and **11a-j** possessing propyl linker on the pyridine ring showed higher inhibitory activity compared to their ethyl linker possessing counterpart **8a-i** and **10a-j**.

In regard to the terminal sulfonamide moiety of methoxy bearing derivatives **8a-i** and **9a-i**, substitution with electron withdrawing groups on compounds **8a** or **9a** had diverse impact on the activity; *para*-substitution with bulky groups such as Br or CF_3 in compounds **8c**, **8h**, **9c**, and **9h** reasonably enhanced the inhibitory, whereas, para or meta substitution with small groups like Cl or F in compounds **8b**, **8d**, **8e**, **8g**, **9b**, **9d**, **9e**, and **9g** dramatically reduced the activity nearly to its half, para OMe substitution in compounds **8i** and **9i** showed no remarkable change in the activity.

However, the hydroxyl owing compounds **10a-j** and **11a-j** responded in a different manner upon substitution on the terminal sulfonamide moiety; in comparison with the unsubstituted derivatives **10a** and **11a**, *para*-substitution with small electron withdrawing group like F or electron donating group OH in compounds **10d**, **10j**, **11d**, and **11j** retain similar inhibitory activity, fierce activity falling was observed by substitution with electron withdrawing groups such as Cl, Br, CF_3, OMe in compounds **10b**, **10c**, **10e**, **10f**, **10g**, **10h**, and **10i**, while compounds **11b**, **11c**, **11e**, **11f**, **11g**, **11h**, **11i** showed moderate activity reduction (Table 2, Fig. 6).

In order to determine the accurate potency of the final target compounds, IC_{50} determination was performed. The test was carried out at 10 doses of tested compounds with serial dilution (3-fold) at 1 μM. An IC_{50} value higher than 1 μM was estimated based on the best curve fitting available. The IC_{50} values were illustrated in Table 3.

Generally, compounds **10a-j** and **11a-j** with *meta* hydroxyl group showed higher potency compared to their methoxy analogue **8a-i** and **9a-i.** In addition, derivatives with propylene spacer between pyridine ring and terminal sulfonamide moieties **11a-j** had higher potency related to compounds having ethylene spacer **10a-j**.

Regarding the first set of compounds **8a-i**, compound **8h** which carries *para* trifluoromethyl benzene sulfonamide had the strongest potency with IC_{50} 1.75 μM followed by *meta* fluoro benzene sulfonamide derivative **8g** with IC_{50} 2.54 μM and *para* bromo benzene sulfonamide derivative **8c** with IC_{50} 3.25 μM. Disubstituted derivative **8f** was more active compared to monosubstituted analogue **8b** with IC_{50s} 8.25 μM and 16 μM, respectively and this different in potency may be related to non-planer effect of disubstituted derivative.

For propylene spacer carrying compounds **9a-i**, slight increase in

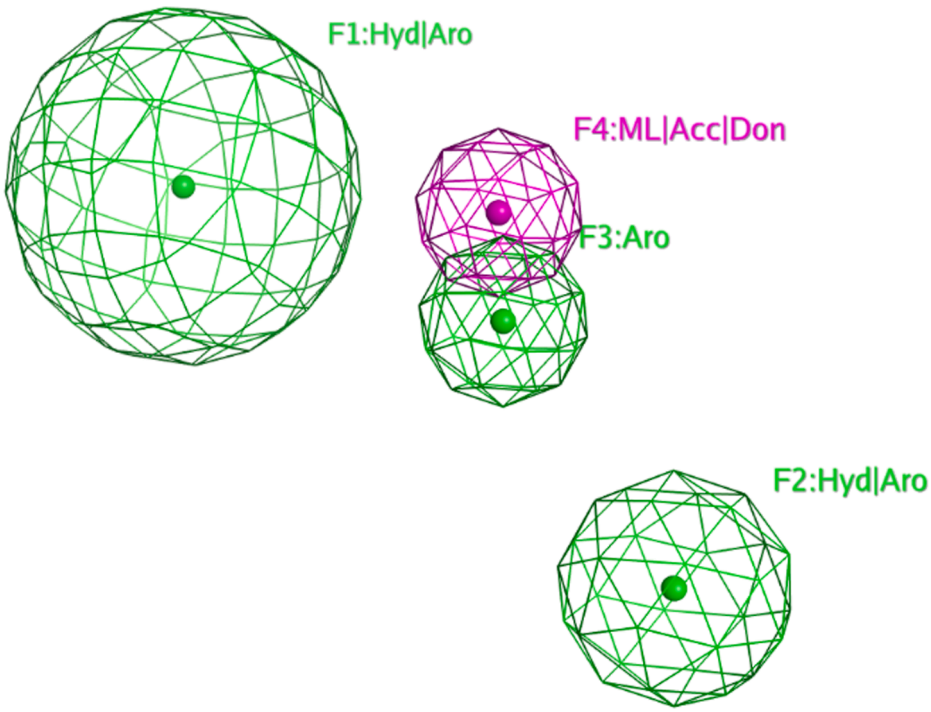

Fig. 4. The common features pharmacophore model generated from training set alignment.

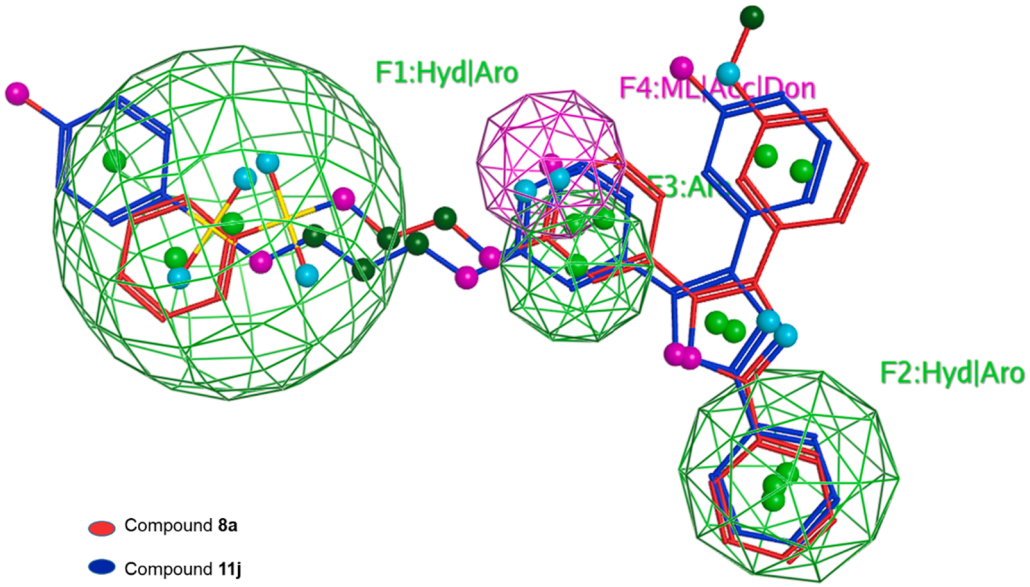

Fig. 5. Mapping of compounds **8a** (red) and **11j** (blue) on the generated pharmacophore model.

potency appeared. Compound **9h** with para trifluoromethyl benzene sulfonamide had the highest activity with IC_{50} 0.98 μM followed by **9g** with IC_{50} 1.15 μM. Compounds 9c and 9d showed similar potencies with IC_{50} 3.52 and 3.91 μM, respectively. *Meta* chloro (6.91 μM) and dichloro substituted (6.75 μM) derivatives had higher activity compared to pare substituted analogue.

Dramatic increase in potency occurred when *meta* methoxy phenyl was replaced with *meta* hydroxyl group **10a-j** and **11a-j**. In addition, unsubstituted derivatives and compounds having small size *para* substitution such as fluoro and hydroxyl group had the highest activity among these derivatives. Compounds **11a** (un substituted with propylene spacer) and **11d** (*para* fluoro with propylene spacer) were emerged to be the most potent inhibitors with IC_{50} values of 47 nm and 45 nm, respectively followed by **10a** (unsubstituted with ethylene spacer) with IC_{50} 95 nM.

2.3.2. *In vitro anti-inflammatory activity*

The anti-inflammatory activity of the active derivatives was detected by their ability to inhibit nitric oxide (NO) and prostaglandin-E2 (PGE2) production by suppression of inducible nitric oxide synthase (iNOS) and cyclooxygenase-2 (COX-2) expression in LPS-stimulated RAW264.7 cells.[45] In addition, the most active inhibitors were evaluated for their effect on inhibiting the production of pro-inflammatory cytokines (TNF-α, 1L-6, and 1L-1β)

2.3.2.1. Nitric oxide (NO) assay. RAW264.7 macrophages were pre-

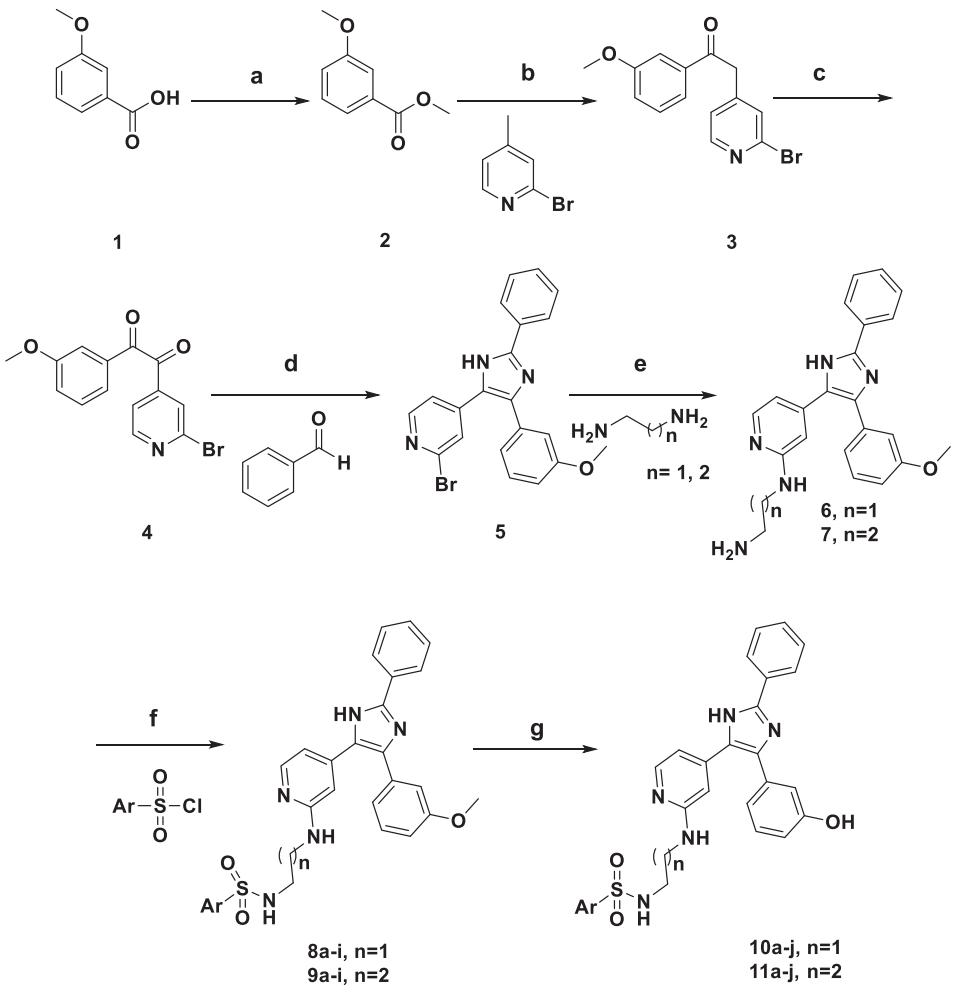

Scheme 1. Reagents and conditions: (a) MeOH, c.H_2SO_4, 80 °C, 12 h.; (b) LiHMDS, THF, −70 °C, 18 h.; (c) HBr, DMSO, 55 °C, 2 h.; (d) NH_4OAC, CH_3COOH, 100 °C, 4 h.; (e) 100 °C, 12 h.; (f) DCM, DIPEA, rt, 12 h.; (g) BBr_3, TBAI, −70 °C, 6 h.

Table 1
Structure of the target compounds **8a-i**, **9a-i**, **10a-j**, and **11a-j**.

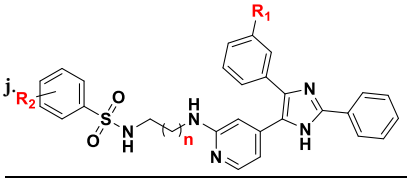

Cpd.	R_1	R_2	n	Cpd.	R_1	R_2	n
8a	OCH_3	H	1	**10b**	OH	p-Cl	1
8b	OCH_3	p-Cl	1	**10c**	OH	p-Br	1
8c	OCH_3	p-Br	1	**10d**	OH	p-F	1
8d	OCH_3	p-F	1	**10e**	OH	m-Cl	1
8e	OCH_3	m-Cl	1	**10f**	OH	2,6-Cl	1
8f	OCH_3	2,6-Cl	1	**10g**	OH	m-F	1
8g	OCH_3	m-F	1	**10h**	OH	p-CF_3	1
8h	OCH_3	p-CF_3	1	**10i**	OH	p-OCH_3	1
8i	OCH_3	p-OCH_3	1	**10j**	OH	p-OH	1
9a	OCH_3	H	2	**11a**	OH	H	2
9b	OCH_3	p-Cl	2	**11b**	OH	p-Cl	2
9c	OCH_3	p-Br	2	**11c**	OH	p-Br	2
9d	OCH_3	p-F	2	**11d**	OH	p-F	2
9e	OCH_3	m-Cl	2	**11e**	OH	m-Cl	2
9f	OCH_3	2,6-Cl	2	**11f**	OH	2,6-Cl	2
9g	OCH_3	m-F	2	**11g**	OH	m-F	2
9h	OCH_3	p-CF_3	2	**11h**	OH	p-CF_3	2
9i	OCH_3	p-OCH_3	2	**11i**	OH	p-OCH_3	2
10a	OH	H	1	**11j**	OH	p-OH	2

Table 2
In vitro p38a kinase % Inhibition data of target compounds **8a-i**, **9a-i**, **10a-j**, and **11a-j**.

Cpd.	% Inhibition of p38α kinase at (10μM)	Cpd.	% Inhibition of p38α kinase at (10μM)
8a	74.42	**10b**	46.60
8b	35.27	**10c**	46.78
8c	90.00	**10d**	97.10
8d	50.01	**10e**	47.86
8e	36.31	**10f**	38.34
8f	34.72	**10g**	59.63
8g	48.61	**10h**	36.50
8h	90.11	**10i**	75.05
8i	61.08	**10j**	99.01
9a	88.61	**11a**	99.80
9b	67.72	**11b**	87.98
9c	94.01	**11c**	87.31
9d	78.95	**11d**	99.70
9e	62.45	**11e**	86.83
9f	65.36	**11f**	81.00
9g	76.42	**11g**	91.00
9h	96.00	**11h**	75.28
9i	89.04	**11i**	92.02
10a	99.70	**11j**	98.01

incubated with different concentrations of the tested compounds for 2 h, and then stimulated by LPS (1 μg/mL) for 24 h. After incubation, the nitrite concentrations of supernatants were determined using Griess reagent.[46] In this study, L-**NIL** (L-N6-(1-iminoethyl) lysine) was used as a

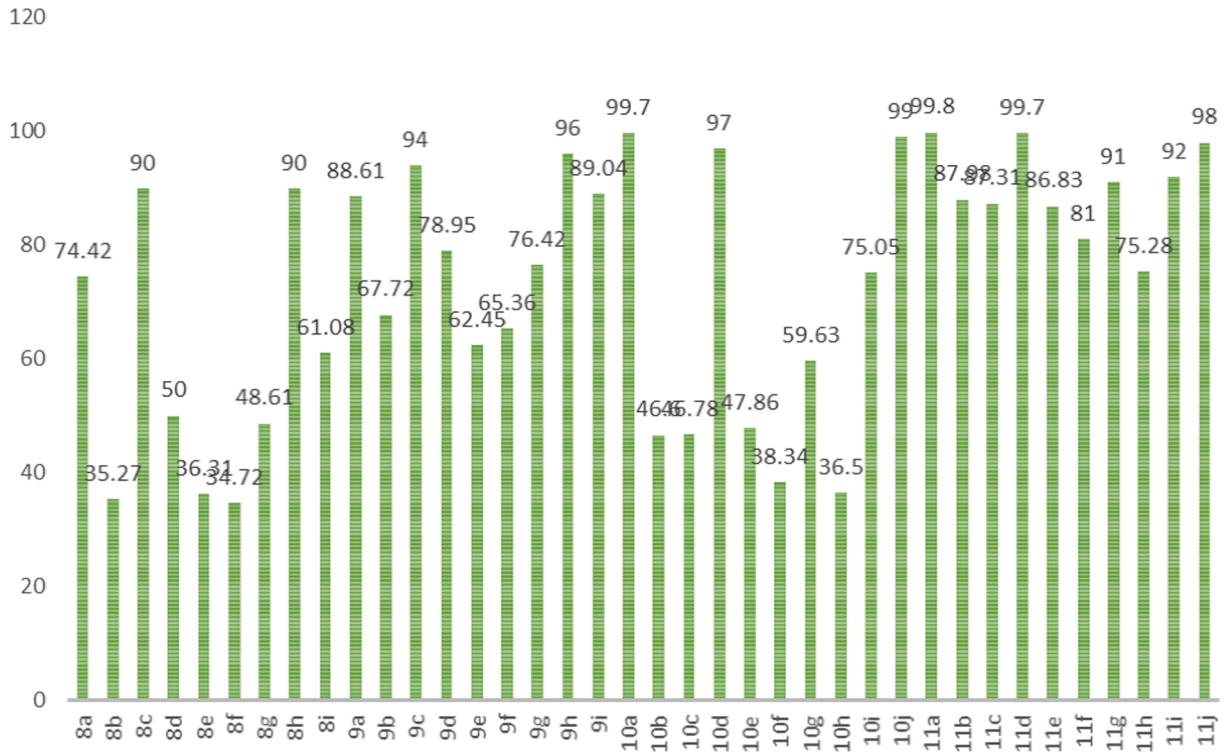

Fig. 6. Inhibitory activities of the target compounds **(8a-i, 9a-i, 10a-j, and 11a**-j) against P38α kinase in terms of percent inhibition.

Table 3
IC_{50} values of final target compounds over p38α/MAPK14 kinase.

Cpd.	P38α kinase IC_{50} (nM)	Cpd.	P38α kinase IC_{50} (nM)
8a	7100 ± 74.00	**10b**	11900 ± 460.00
8b	16000 ± 122.00	**10c**	12100 ± 395.00
8c	3250 ± 125.00	**10d**	**150±23.20**
8d	10000 ± 255.00	**10e**	10200 ± 246.00
8e	14500 ± 350.00	**10f**	14300 ± 742.00
8f	8250 ± 210.00	**10g**	8950 ± 460.00
8g	2540 ± 360.00	**10h**	13210 ± 578.00
8h	1750 ± 150.00	**10i**	2160 ± 199.00
8i	8720 ± 348.00	**10j**	510 ± 5.21
9a	4980 ± 416.00	**11a**	**47±1.16**
9b	7850 ± 201.00	**11b**	**120±6.51**
9c	3520 ± 310.00	**11c**	**99±2.36**
9d	3910 ± 275.00	**11d**	**45±0.98**
9e	6910 ± 175.00	**11e**	101 ± 2.22
9f	6750 ± 190.00	**11f**	8250 ± 35.5
9g	1150 ± 285.00	**11g**	321 ± 3.14
9h	980 ± 25.00	**11h**	961 ± 65.00
9i	4120 ± 142.00	**11i**	130 ± 4.56
10a	**95±4.21**	**11j**	124 ± 5.44

reference compound at concentration of 40 μM, L-NIL is a potent and selective inhibitor of inducible nitric oxide synthase (**iNOS**) over other nitric oxide synthase isoforms.[47]

The nitric oxide inhibitory activity at fixed concentration (1 μM) and IC_{50} for the final target compounds were represented in Table 4. Compounds **9c, 9d, 9h 10a, 11a, 11b, 11c, 11i** and **11j** exhibited the highest activity with percent inhibition 72%, 69%, 70%, 71% 72%, 74%, 73%, 71% and 72%, and IC_{50s} 0.62 μM, 0.94 μM, 0.71 μM, 0.62 μM, 0.58 μM, 0.51 μM, 0.50 μM, 0.68 μM and 0.66 μM, respectively.

The data in Fig. 7 reveals that a significant raise in nitric oxide concentration was noticed after stimulation of the cell lines with LPS in comparison with the LPS non-stimulated blank cells, the concentration of NO was reduced to its half in the cells which previously incubated with L-NIL. While, the most potent P38α inhibitors **9c**, **10a**, **11b**, **11d**,

Table 4
Nitric oxide percent inhibition at 1 μM for final target compounds and their IC_{50} in LPS-stimulated RAW264.7 cells.

Cpd.	NO % inhibition	IC_{50} (μM)	Cpd.	NO % inhibition	IC_{50} (μM)
8a	17.81% ± 1.21	10.21 ± 1.20	**10b**	38.26% ± 1.33	2.98 ± 0.09
8b	9.61% ± 1.02	20.35 ± 2.48	**10c**	28.37% ± 0.99	6.35 ± 0.06
8c	37.65% ± 2.10	6.35 ± 0.98	**10d**	60.21% ± 1.61	0.71 ± 0.002
8d	21.56% ± 0.99	9.84 ± 0.62	**10e**	21.96% ± 0.74	5.32 ± 0.08
8e	12.65% ± 0.88	19.81 ± 1.06	**10f**	29.11% ± 2.11	4.55 ± 0.03
8f	25.36% ± 1.18	9.67 ± 0.87	**10g**	37.34% ± 0.85	3.92 ± 0.09
8g	40.55% ± 1.45	4.89 ± 0.71	**10h**	40.32% ± 1.46	3.99 ± 0.07
8h	45.32% ± 1.68	3.12 ± 0.45	**10i**	51.25% ± 0.97	0.99 ± 0.01
8i	13.64% ± 0.96	9.96 ± 0.74	**10j**	62.33% ± 1.08	0.68 ± 0.01
9a	26.53% ± 2.22	6.35 ± 0.61	**11a**	72.56% ± 0.87	0.58 ± 0.01
9b	60.21% ± 1.77	0.85 ± 0.01	**11b**	74.29% ± 0.82	0.51 ± 0.01
9c	72.18% ± 1.35	0.62 ± 0.03	**11c**	75.25% ± 0.88	0.50 ± 0.02
9d	69.52% ± 0.85	0.94 ± 0.06	**11d**	69.28% ± 1.31	0.61 ± 0.02
9e	48.56% ± 0.96	1.01 ± 0.02	**11e**	65.32% ±1.35	0.67 ± 0.02
9f	56.54% ± 1.31	0.92 ± 0.01	**11f**	42.25% ±1.42	1.17 ± 0.06
9g	61.35% ± 2.14	0.88 ± 0.01	**11g**	54.27% ± 0.52	0.86 ± 0.03
9h	70.02% ± 0.77	0.71 ± 0.01	**11h**	44.31% ± 0.67	2.64 ± 0.07
9i	63.54% ± 0.81	0.83 ± 0.004	**11i**	71.28% ± 0.89	0.68 ± 0.01
10a	71.55% ± 1.47	0.62 ± 0.003	**11j**	72.42% ± 1.00	0.66 ± 0.01

and **11j** showed a slight reduction in NO production at concentration of 10 nm, a significant fall in NO concentration was observed in cells incubated with 100 nm and 1000 nm of compound **11j**.

2.3.2.2. PGE_2 enzyme-linked immunosorbent assay. RAW264.7 cells were incubated with LPS (1 μg/mL) for 24 h. PGE2 levels were analyzed using the prostaglandin E2 BiotrackELISA system.[48] In this test, **NS-398** was used as a reference compound, NS-398 is a novel anti-inflammatory

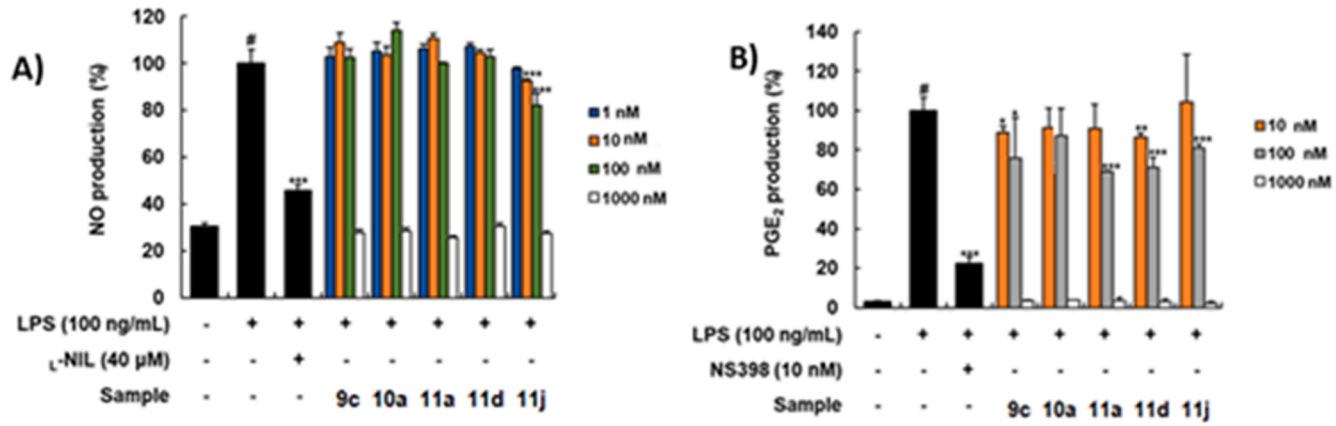

Fig. 7. (A) Nitric oxide production inhibition activity of compounds **9c**, **10a**, **11a**, **11d**, and **11j** on LPS stimulated RAW 264.7 macrophage (B) PGE2 production inhibition activity of compounds **9c**, **10a**, **11a**, **11d**, and **11j** on LPS stimulated RAW 264.7 macrophage.

and analgesic agent that inhibits prostaglandin production through the inhibition of cyclooxygenase-2 (COX-2) activity.[49]

Compounds **8g** and **8h** were the most potent compounds among the first series **8a-i** with percent inhibition 78.22% and 78.25% and IC_{50s} 0.630 μM and 0.634 μM. On the other hand, compounds **9c, 9d** and **9h** were the most potent compounds in the second series with percent inhibition 97%, 92% and 95% and IC_{50s} 0.551 μM, 0.541 μM, and 0.523 μM, respectively. Regarding the third series **10a-j**, compounds **10a** and **10d** showed the highest activities with percent inhibition 96% and 95% and IC_{50s} 0.520 and 0.310 μM. Compounds **11a**, **11b**, **11c**, **11d**, **11e** and **11j** showed over 90% inhibition at 1 μM and IC_{50s} 0.312, 0.589, 0.601, 0.290, 0.581 and 0.546 μM (Table 5).

The data in Fig. 7 illustrates that remarkable jump in PGE2 production was observed upon treatment with LPS, the concentration of PGE2 was dramatically declined to its fifth by incubation with NS-398. At concentration 10 nm, the most potent compounds **9c**, **10a**, **11a**, **11d**, and **11j** were obviously ineffective in reducing PGE2 production. However, by raising the concentration of the tested compounds to 100 and 1000 nM dramatic decrease in PGE2 was observed.

2.3.2.3. Inflammatory cytokines production assay. Further investigation was conduct to the most potent P38α inhibitor compounds **11d** and **11a** were further evaluated for inhibitory effect on the proinflammatory cytokines TNF-α, 1L-6, and 1L-1β production in lipopolysaccharide-stimulated THP-1 human cells (Fig. 8). Compound **11d** showed high potency against the production of TNF-α and 1L-1β with IC_{50} values of 78 nM and 82 nM, respectively. While the production of 1L-6 was moderately inhibited by higher concentration of compound **11d** (IC_{50} = 17.6 μM). Compound **11a** showed good activity against TNF-α production (IC_{50} = 98.02 nM), but showed no remarkable activity against the production of 1L-6 and 1L-1β.

2.4. Molecular modelling studies

2.4.1. Molecular docking study

In attempt to correlate the diversity in p38α/MAPK14 kinase inhibitory activities and the Imidazolyl pyridine compounds structural features, Molecular docking was performed using (MOE) software. Target compounds **8a-i**, **9a-i**, **10a-j**, and **11a-j** were docked inside the active site of p38α/MAPK14 kinase in complex with **SB203580** (PDB ID: 3GCP)[35] in order to define their binding pattern (**Table S1**). The obtained docking results show that the SB203580-p38α/MAPK14 kinase domain complex has a low root mean square deviation, RMSD (1.0579) that proves valid docking protocol with dock score (−12.16 kcal/mol, Table 3). The native ligand (**SB203580**) binds in the ATP pocket through H-bond formation between the Nitrogen of pyridine ring at position 5 of the imidazole ring and Met109 amino acid in the adenine hinge region,

Table 5
Percent inhibition of PGE2 at 1 μM for final target compounds and their IC_{50} in LPS-stimulated RAW264.7 cells.

Cpd.	%Inhibition of PGE_2	IC_{50} (nM)	Cpd.	%Inhibition of PGE_2	IC_{50} (nM)
8a	77.23% ± 1.32	643.21 ± 5.17	**10b**	81.89% ± 0.95	612.25 ± 6.33
8b	69.31% ± 2.11	716.54 ± 4.72	**10c**	58.41% ± 0.86	920.67 ± 15.21
8c	61.36% ± 3.15	810.36 ± 8.31	**10d**	**95.68% ± 1.05**	310.11 ± 9.35
8d	62.12% ± 3.51	797.71 ± 7.38	**10e**	60.21% ± 0.98	756.38 ± 13.61
8e	59.66% ± 2.84	838.86 ± 5.89	**10f**	59.25% ± 1.18	795.32 ± 9.15
8f	66.61% ± 2.98	742.38 ± 4.68	**10g**	69.78% ± 0.88	698.58 ± 11.23
8g	78.22% ± 1.33	634.37 ± 6.35	**10h**	71.27% ± 0.94	670.54 ± 10.27
8h	78.52% ± 2.37	630.65 ± 7.61	**10i**	87.69% ± 0.71	565.89 ± 5.66
8i	55.25% ± 1.87	901.11 ± 11.25	**10j**	89.65% ± 0.84	530.24 ± 8.99
9a	79.21% ± 2.42	625.16 ± 9.57	**11a**	**96.43% ± 1.41**	312.39 ± 4.32
9b	88.36% ± 3.21	561.21 ± 4.95	**11b**	**91.26% ± 1.27**	589.28 ± 6.54
9c	**97.14% ± 1.60**	511.35 ± 4.21	**11c**	**90.99% ± 1.01**	601.21 ± 7.89
9d	**92.35% ± 1.99**	541.76 ± 8.64	**11d**	**96.93% ± 1.11**	290.42 ± 5.14
9e	85.32% ± 1.54	581.68 ± 7.89	**11e**	**92.35% ± 0.84**	581.56 ± 4.98
9f	86.65% ± 1.16	577.71 ± 6.25	**11f**	74.65%± 0.71	797.58 ± 8.74
9g	89.35% ± 1.56	556.52 ± 5.35	**11g**	86.88% ± 0.93	625.54 ± 7.11
9h	**95.41% ± 2.01**	523.35 ± 4.58	**11h**	87.58%±0.61	618.21 ± 8.16
9i	71.59% ±1.97	690.49 ± 9.12	**11i**	89.47%± 0.86	601.54 ± 7.17
10a	**96.28% ± 0.05**	520.94 ± 4.57	**11j**	**92.57% ± 0.80**	546 ± 3.75

while, the hydrophobic back pocket is occupies by the 4-fluoro phenyl moiety at position 5 of the imidazole ring, the central imidazole ring embeds in the ribose pocket via arene-H-bond interaction with Val38, the oxygen of the terminal methylsulfinyl phenyl at position 2 of the imidazole ring binds in the phosphate area by forming H-bond with Tyr35 residue.

Accordingly, the target compounds were proposed to conserve the essential binding behavior of SB203580. Analysis of the docking results

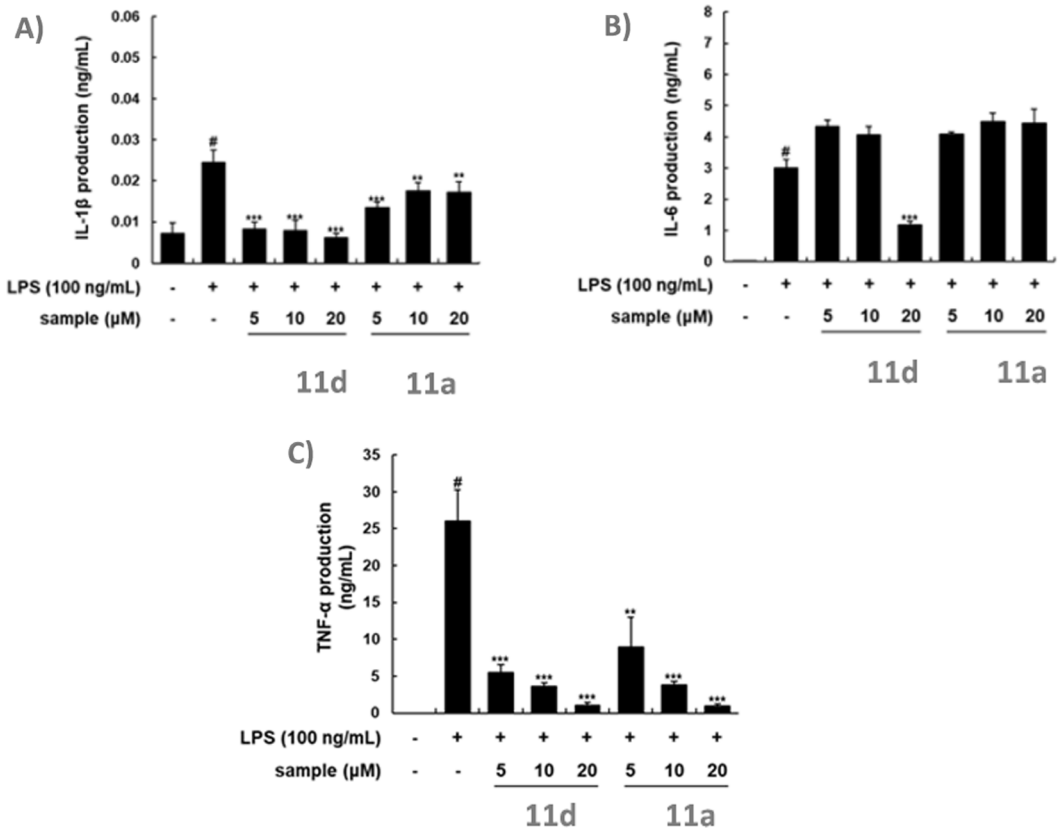

Fig. 8. Effect of **11d** and **11a** on cytokine production in LPS-stimulated Raw 264.7 macrophage at different concentration. (A) 1L-1β (ng/mL) (B) 1L-6 (ng/mL). (**C**) TNF-α (ng/mL).

in Table 6 revealed that most of the target compounds bind in the hinge region by the same manner of SB203580 when NH of Met109 binds to the nitrogen of the pyridine via a H-bond, besides, well alignment is observed between Imidazole scaffold of the target compounds and SB203580 imidazole where the N-3 of imidazole form H-bond with Lys53 in the sugar binding area (Fig. 9). Interestingly, imidazole ring in some derivatives with a high binding score exhibit different binding mode through arene-arene interaction with Phe169 in compounds **8h**, **10d**, **11a**, **11f**, and **11i**. Additional molecular interactions are noticed in compounds **8a**, **8b**, **8c**, **8e**, **8i**, **9c**, **10b**, **10e**, **10i**, **10j**, **11c**, and **11e** because of the terminal sulfonamide moiety with ethyl or propyl linker, the oxygen of sulfonamides shares by H-bond with Cys172 which results in orientation of the aromatic groups towards the hydrophobic front pocket. Moreover, Arene-H interactions are formed between the terminal aromatic moiety of sulfonamides and amino acids Cys172, Thr185, and Gly110 in compounds **8f**, **8h**, and **9b**, respectively (Fig. 9).

2.4.2. Molecular dynamics simulations

From the previous docking findings, the most potent inhibitor compound **11d** showed high fitting affinity in the active site of P38α kinase with energy score of −12.79 Kcal/mole, while the native ligand energy was −12.19 Kcal/mole (Fig. 10). Compound **11d** binds into the kinase active site by two H-bonds with Lys53 backbone, one additional H-bond was formed between the terminals 3-hydroxy phenyl moiety and His107 residue. In addition, the central imidazole ring embedded in the ribose pocket via Arene-H interaction with Val38, the phenyl group at the imidazole position 2 participated in Arene-H interaction with Tyr35. Finally, water molecules formed a bridge of interaction between NH of Imidazole ring and Leu171, and 4-fluoro phenyl moiety and Arg67.

Accordingly, molecular dynamics (MD) simulations analysis was conducted for compound **11d** in a bid to study the conformational stability of its docked inhibitor-protein complex and to attain dependable drug-receptor–binding affinities.

MD simulations study was performed for 600 ns for inhibitor **11d** in comparison to the native ligand **SB203580** in the active site of the corresponding kinase (PDB ID: 3GCP). The MD simulations protocol was run at 300 K temperature, and the atomic potential energy was recorded in a time interval of 0.5 ns.

To explore the dynamic stability of both 3GCP-**11d** and 3GCP-**SB203580** complexes, the time-dependent atomic potential energy of each complex was calculated during MD trajectories. As illustrated in Fig. 11, the ligand-protein complex (3GCP/**SB203580**) attained the equilibrium around 250 ns. While, the inhibitor-protein complex (3GCP/**11d**) achieved equilibrium around 300 ns.

In addition, the root mean square deviation (RMSD) values were observed during the simulation process to predict the stability of the ligand-protein complex. The recorded RMSD values were also represented as a function of time in Fig. 12. The obtained results indicate that the native ligand and the tested inhibitor **11d** have retained their binding affinity and kept firmly bound to their respective kinase binding site. As shown in Fig. 12, the inhibitor-protein and ligand-protein complexes exhibited interaction stability during the first 300 ns of simulations. Then, RMSD curves of the tested ligands fluctuated for around 100 ns of simulation before its quite stability at the end of simulation time 600 ns.

3. Structure activity relationship

The final target compounds exhibited structural diversity included different substitutions and different spacer length, which in turn bring each derivative a different structural features. As a result, broad range of the inhibitory activity was obtained over treating the enzyme with a dose of corresponding compound. Such a variability in compounds activities is illustrated in (Fig. 13) as following; 1) An elevation of P38α

Table 6
Docking results of target compounds **8a-i**, **9a-i**, **10a-j**, and **11a-j** in p38α/MAPK14 kinase (PDB ID: 3GCP).

Comp.	Energy score (Kcal/mol)	Amino acid	Binding group	Interaction	H- bond length (Å)
SB203580	−12.16	Met109	Pyridine ring (N)	H-bond	2.73
		Tyr35	SOCH3 (O)	H-bond	2.51
		Val38	Imidazole ring	Arene-H	
8a	−13.87	Lys53	Imidazole ring (N)	H-bond	3.47
		Met109	Pyridine ring (N)	H-bond	3.47
		Cys172	SO2	H-bond	3.95
8b	−12.52	Lys53	Imidazole ring (N)	H-bond	3.32
		Met109	Pyridine ring (N)	H-bond	3.57
		Cys172	SO2	H-bond	3.96
8c	−12.19	Lys53	Imidazole ring (N)	H-bond	3.32
		Met109	Pyridine ring (N)	H-bond	3.58
		Cys172	SO2	H-bond	3.93
8d	−13.42	Met109	Pyridine ring (N)	H-bond	3.39
8e	−12.07	Cys172	SO2	H-bond	3.95
8f	−11.49	Lys53	Imidazole ring (N)	H-bond	3.52
		Met109	Pyridine ring (N)	H-bond	3.41
		Cys172	2,6-Cl-Phenyl ring	Arene-H	
8g	−12.87	Lys53	HN-SO2 (NH)	H-bond	2.98
8h	−13.05	Lys152	SO2	H-bond	3.63
		Phe169	Imidazole ring	Arene-Arene	
		Thr185	4-CF3-Phenyl ring	H-bond	2.98
8i	−11.84	Lys53	Imidazole ring (N)	H-bond	2.85
		Cys172	SO2	H-bond	3.44
		Phe169	Imidazole ring	Arene-Arene	
		Val38	Pyridine ring	Arene-H	
9a	−15.52	Lys53	SO2	H-bond	3.45
		Gly110	Phenyl ring	Arene-H	
		Val38	Pyridine ring	Arene-H	
9b	−13.15	Gly110	4-Cl-Phenyl ring	Arene-H	3.41
		Met109	Pyridine ring (N)	H-bond	
9c	−13.19	Cys172	HN-SO2 (NH)	H-bond	4.29
		Met109	Pyridine ring (N)	H-bond	3.34
9d	−13.74	Met109	Pyridine ring (N)	H-bond	3.3
9e	−12.20	Val38	Imidazole ring	Arene-H	
9f	−12.81	Phe169	Imidazole ring	Arene-Arene	
9g	−14.42	Met109	Pyridine ring (N)	H-bond	3.49
9h	−13.19	Phe169	Imidazole ring	Arene-Arene	
9i	−12.23	Lys53	Imidazole ring (N)	H-bond	3.42
10a	−14.09	Lys53	Imidazole ring (N)	H-bond	3.3
		Met109	Pyridine ring (N)	H-bond	3.48
		Cys172	SO2	H-bond	3.89
10b	−13.23	Met109	Pyridine ring (N)	H-bond	3.58
		Cys172	SO2	H-bond	3.39
10c	−12.52	Met109	Pyridine ring (N)	H-bond	3.47
10d	−13.78	Lys53	Imidazole ring (N)	H-bond	2.89
		Phe169	Imidazole ring	Arene-Arene	
10e	−13.60	Cys172	SO2	H-bond	3.9
		Lys53	HN-SO2 (NH)	H-bond	4.12
		Phe169	Imidazole ring (N)	H-bond	3.02
			Imidazole ring	Arene-Arene	
10f	−13.54	Met109	Pyridine ring (N)	H-bond	3.44
10g	−13.96	Met109	Pyridine ring (N)	H-bond	3.44
10h	−12.80	Met109	Pyridine ring (N)	H-bond	3.39
10i	−14.86	Lys53	Imidazole ring (N)	H-bond	3.26
		Met109	Pyridine ring (N)	H-bond	3.51
		Cys172	SO2	H-bond	4.15
10j	−13.09	Met109	Pyridine ring (N)	H-bond	3.32
		Cys172	SO2	H-bond	3.95
11a	−12.64	Lys53	Imidazole ring (N)	H-bond	3.31
		Leu171	HN-SO2 (NH)	H-bond	3.47
		Phe169	Imidazole ring	Arene-Arene	
11b	−12.31	Lys53	Imidazole ring (N)	H-bond	2.85
		Phe169	Imidazole ring	Arene-Arene	
11c	−14.55	Met109	Pyridine ring (N)	H-bond	3.56
		Cys172	SO2	H-bond	3.48
11d	−12.79	His107	3-OH phenyl (OH)	H-bond	2.51
		Lys53	SO2	H-bond	2.53
		Tyr35	NH	H-bond	2.92
		Val38	Phenyl ring	Arene-H	
			Imidazole ring	Arene-H	
11e	−13.45	Met109	Pyridine ring (N)	H-bond	2.91
		Cys172	SO2	H-bond	3.49
				H-bond	3.54
11f	−12.56	Lys53	Imidazole ring (N)	H-bond	2.78
		Phe169	Imidazole ring	Arene-Arene	
		Val38	Pyridine ring	Arene-H	
11g	−13.45	Leu171	HN-SO2 (NH)	H-bond	3.16
		Met109	Pyridine ring (N)	H-bond	4.2
11h	−12.47	Lys53	Imidazole ring (N)	H-bond	3.45
		Met109	Pyridine ring (N)	H-bond	3.44
11i	−12.50	Lys53	Imidazole ring (N)	H-bond	3.41
		Met109	Pyridine ring (N)	H-bond	3.54
		Phe169		Arene-Arene	

(*continued on next page*)

Table 6 (*continued*)

Comp.	Energy score (Kcal/mol)	Amino acid	Binding group	Interaction	H- bond length (Å)
11j	−14.02	Met109	Imidazole ring Pyridine ring (N)	H-bond	3.27

kinase inhibitory activity was observed upon demethylation of compounds **8a-i** and **9a-i** to their corresponding meta hydroxyl derivatives **10a-j** and **11a-j**, the produced hydroxyl moiety might improve the solubilisation of the compounds and increase their affinity in the enzyme binding pocket by providing additional H-bond. 2) Additionally, the propylene linker in compounds **9a-i** and 1**1a-j** allows the extension of the terminal aromatic sulphonamide moiety into the front hydrophobic pocket of P38α kinase, and resulting in higher potency comparing to the ethylene linker owing derivatives **8a-i** and **10a-j**. 3) Regarding to the terminal aromatic sulphonamides, substitution on the phenyl group didn't show significant impact on the activity except for the *para*-fluoro substituted derivatives with the propylene linker (**9d** and **11d**), while, bulky group substitution dramatically declined the activity.

4. Conclusion

A group of off-target based drug repurposing strategies were followed to repositioning of a series of 38 imidazoly pyridine B-RAF^{V600E} kinase inhibitors to work as p38α kinase inhibitors. Protein alignment protocol was applied to superpose the crystal structures of p38α kinase (PDB: 3GCP) and B-RAF^{V600E} kinase (PDB: 4XV2), and the ligand binding site of both enzymes showed high sequence similarities. Therefore, SB203580 the native ligand of p38α kinase (PDB: 3GCP) was used as a lead compound to predict the binding mode of the target compound and their expected activity, as well. Furthermore, pharmacophore model was built using a group of 25 p38α kinase inhibitors with a wide range of inhibitory activity, the produced model was used for mapping the target derivatives in order to prove their fitting affinity, the tested compounds exhibited typical fitting in the model. The target compounds were evaluated for their potency to inhibit p38α kinase, compounds **11a** and **11d** emerged to be the most potent inhibitors (IC_{50} = 47 nm and 45 nm, respectively). Compound **11d** was subjected to further investigation in order to determine its prolonged effect on the production of pro-inflammatory cytokines (TNF-α, 1L-6, and 1L-1β) in LPS-stimulated RAW264.7 macrophages. Compound **11d** showed high potency against the production of TNF-α, 1L-6, and 1L-1β with IC_{50}

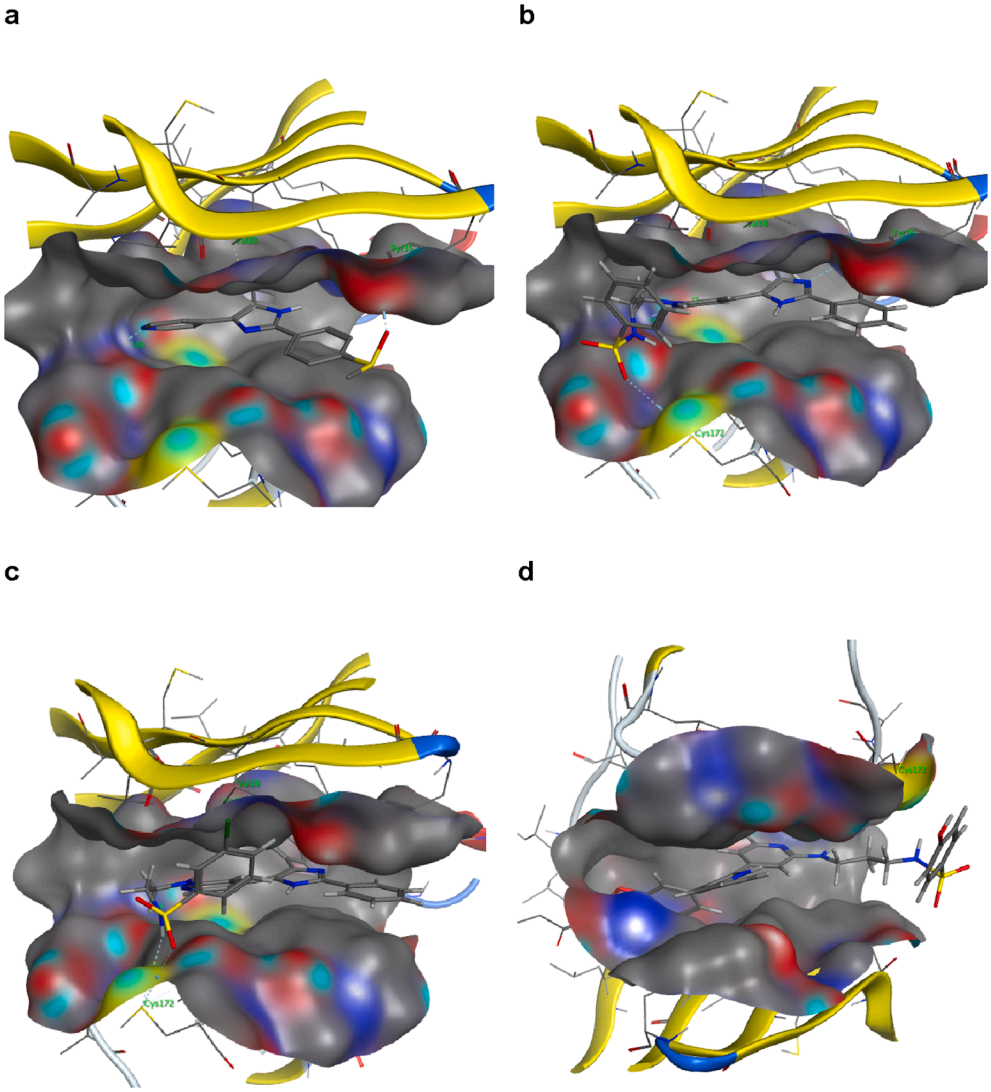

Fig. 9. 3D representation of docking study output (PDB ID: 3GCP). (a) 3D interaction of **SB203580** (native ligand) with p38α/MAPK14 kinase enzyme domain; (b) 3D interaction of **8a** with p38α/MAPK14 kinase enzyme domain; (c) 3D interaction of **10e** with p38α/MAPK14 kinase enzyme domain; (d) 3D interaction of **11j** with p38α/MAPK14 kinase enzyme domain.

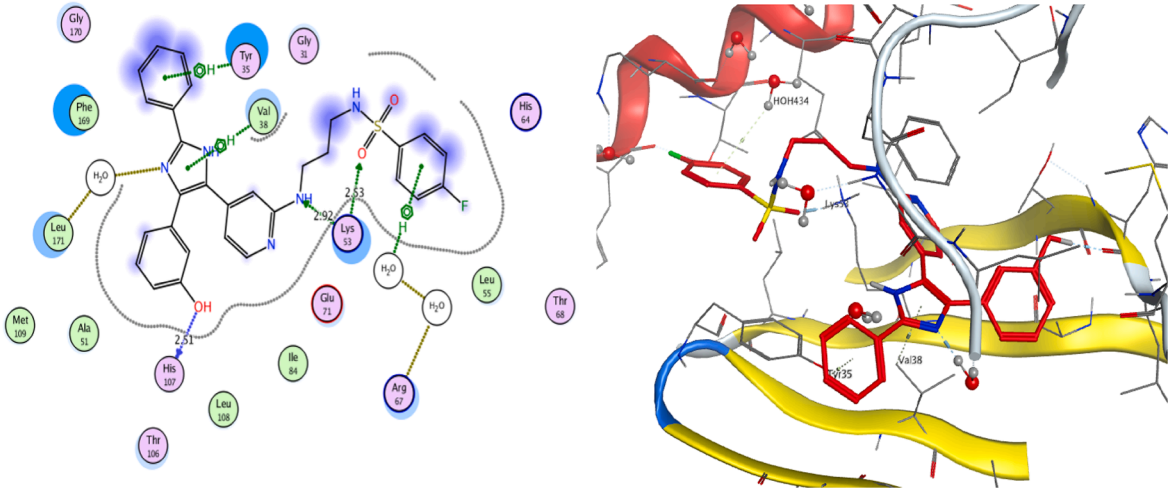

Fig. 10. 2D and 3D interaction diagram of compound 11d in the active site of P38α kinase (PDB ID: 3GCP).

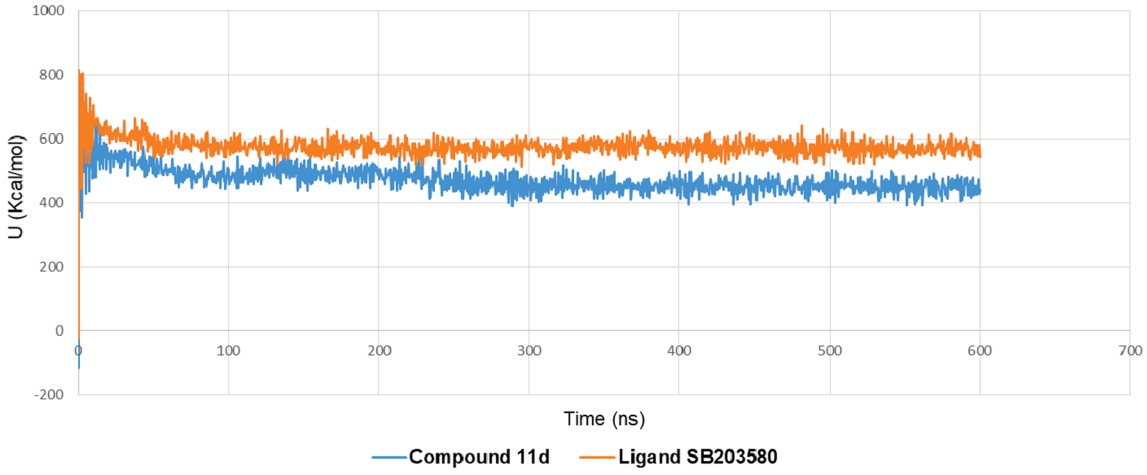

Fig. 11. Potential energy evaluation of complex of compound **11d** and native ligand **SB203580** with P38α kinase (PDB ID: 3GCP) binding site as function of time (ns).

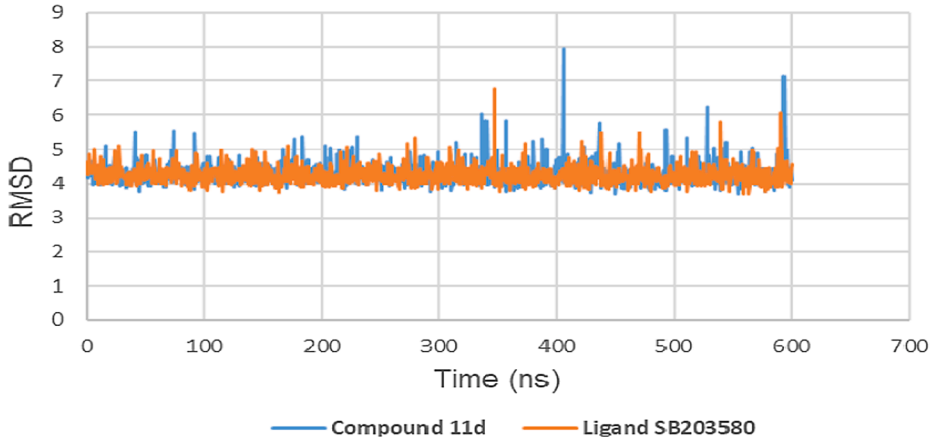

Fig. 12. The RMSD curve from the molecular dynamics simulation of compound **11d** and native ligand **SB203580** complexes with P38α kinase. The x-axis represents the simulation time (ns), while the y-axis represents the RMSD value (nm).

values of 78 nM, 17.6 μM, and 82 nM, respectively.

Moreover, the anti-inflammatory activity of was detected by determining the ability of the target compounds to inhibit nitric oxide (NO) and prostaglandin-E2 (PGE2) in LPS-stimulated RAW264.7, compound **11d** exhibited satisfied inhibitory activity of the production of PGE2 and NO with IC_{50} values of 3.8 μM and 8.4 μM, respectively.

To correlate the enzyme activity of the target compounds with their structure, the compounds were docked into the p38α kinase crystal

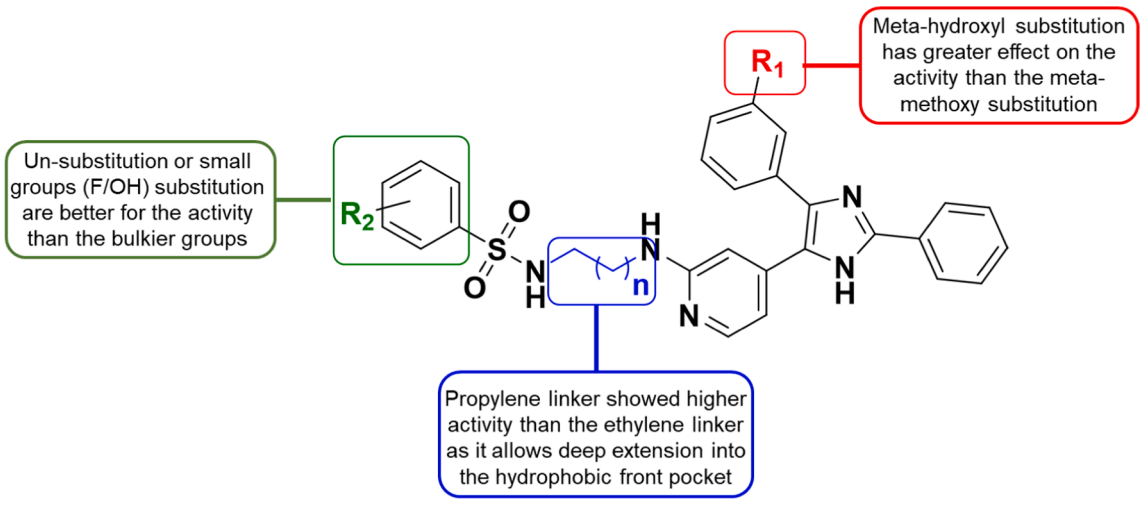

Fig. 13. Structural activity relationship of the target compounds illustrating the effect of their structural features and the enzyme inhibitory activity.

structure (PDB: 3GCP), most of the derivatives conserved the same binding behavior of the native ligand SB203580. In addition, the conformational stabilities of the protein–ligand complexes obtained via docking of the potent inhibitor **11d** and the native ligand were studied by applying MD simulations protocol, the potential energy was calculated during the stimulation process in a time interval of 0.5 ns for 600 ns.

The currently investigated imidazoly pyridine series is considered a starting point for further structural modification in developing potent p38α kinase inhibitors with promising anti-inflammatory activity.

5. Experimental

5.1. Chemistry

The intermediate compounds as well as the target compounds were purified by flash column chromatography using silica gel 60 (0.040–0.063 mm, 230–400 mesh ASTM) and technical grade solvents. ^{1}H NMR and ^{13}C NMR analyses were carried out on a Bruker Avance 400 spectrometer using tetramethylsilane (TMS) as an internal standard. Melting points were measured on a Walden Precision Apparatus Electrothermal 9300 apparatus and were uncorrected. LC-MS analysis was conducted using the following system: Waters 2998 photodiode array detector, Waters 3100 mass detector, Waters SFO system fluidics organizer, Waters 2545 binary gradient module, Waters reagent manager, Waters 2767 sample manager, Sunfire™ C^{18} column (4.6 × 50 mm, 5 µm particle size); Solvent gradient = 95% A at 0 min, 1% A at 5 min; solvent A: 0.035% trifluoroacetic acid (TFA) in water; solvent B: 0.035% TFA in MeOH; flow rate = 3.0 mL/min; the AUC was calculated using Waters MassLynx 4.1 software. The solvents and liquid reagents were transferred using hypodermic syringes. All the solvents and reagents were purchased from commercial companies, and used as such.

5.1.1. Methyl 3-methoxybenzoate (2)

A mixture of 3-methoxybenzoic (**1**, 4.24 g, 0.002 mol) and methanol (40 mL) were heated under reflux until the benzoic acid was dissolved in methanol then few drops of concentrated sulphuric acid was added to the mixture and refluxed for 8 h. The resulting mixture was cooled to room temperature, diluted with water and a saturated solution of sodium bicarbonate was added to the mixture to neutralize the benzoic acid, extracted with ethyl acetate, dried and evaporated to get the required ester compound **2**.

Yield: 90%. m.p.: 110–112 °C. ^{1}H NMR (400 MHz, $CDCl_3$) δ 7.61 (m, 1H, Ar-H), 7.54 (m, 1H, Ar-H), 7.31 (t, J = 8 Hz, 1H, Ar-H), 7.07 (m, 1H, Ar-H), 3.89 (s, 1H, OOCH3), 3.81 (s, 1H, OCH3). ^{13}C NMR (100 MHz, CDCl3) δ 166.85 (Ar-C), 159.86 (Ar-C), 131.41 (Ar-C), 129.6 (Ar-C), 122.16 (Ar-C), 119.36 (Ar-C), 114.22 (Ar-C), 55.29 (OOCH3), 52.04 (OCH3).

5.1.2. 2-(2-Bromopyridin-4-yl)-1-(3-methoxyphenyl)ethan-1-one (3)

A solution of compound **2** (1.0 g, 5.0 mmol) and 2-bromo-4-picoline (0.5 mL, 5.6 mmol) in THF (5 mL) was cooled to −25 °C, and LiHMDS (3.7 mL, 1.0 M solution in THF, 19.9 mmol) was slowly added at −25 °C to the reaction mixture maintaining the temperature at −25 °C. The resulting mixture was stirred overnight at room temperature. The mixture was quenched with saturated aqueous NH_4Cl (15 mL), and ethyl acetate (20 mL) was added. The organic layer was separated, and the aqueous layer was extracted with ethyl acetate (3–10 mL). The combined organic layer was washed with saline and dried over anhydrous sodium sulfate. The organic solvent was evaporated under vacuum and the residue was purified by flash column chromatography (silica gel, hexane ethyl acetate 1:1 v/v then switching to hexane-ethyl acetate 1:5 v/v) to yield the title compound 4, which was subjected to the next step without further purification.

5.1.3. 1-(2-Bromopyridin-4-yl)-2-(3-methoxyphenyl)ethane-1,2-dione (4)

A solution of compound **4** (2.0 g, 6.8 mmol) in DMSO (10 mL) was heated to 55 °C. Hydrobromic acid (2.5 mL, 20.4 mmol, 3 eq.) was added dropwise to the reaction mixture. The reaction was stirred at 55 °C for 2 h. The reaction mixture was poured carefully to a saturated solution of sodium bicarbonate, extracted with ethyl acetate, dried and evaporated to get the required compound **4**.

Yield: 80%. m.p.: 115–117 °C. ^{1}H NMR (400 MHz, $CDCl_3$) δ 8.63 (d, J = 5.2 Hz, 1H, Ar-H), 7.97 (s, 1H, Ar-H), 7.75 (d, J = 1.2 Hz, 1H, Ar-H), 7.74 (d, J = 1.2 Hz, 1H, Ar-H), 7.48 (m, 2H, Ar-H), 7.26 (m, 1H, Ar-H), 3.9 (s, 3H, OCH_3). ^{13}C NMR (100 MHz, $CDCl_3$) δ 191.71 (Ar-C), 191.01 (Ar-C), 160.26 (Ar-C), 151.57 (Ar-C), 143.47 (Ar-C), 141.19 (Ar-C), 133.25 (Ar-C), 130.3 (Ar-C), 127.24 (Ar-C), 123.39 (Ar-C), 122.65 (Ar-C), 121.26 (Ar-C), 113.08 (Ar-C), 55.61 (OCH_3).

5.1.4. 2-Bromo-4-(4-(3-methoxyphenyl)-2-phenyl-1H-imidazol-5-yl) pyridine (5)

To a solution of compound **4** (1.23 g, 4 mmol) and Benzaldehyde (0.4 mL, 4 mmol) in acetic acid (10 mL), ammonium acetate (3.1 g, 40 mmol, 10 eq.) was added. The reaction mixture was heated to 100 °C for 4 h. The reaction mixture was poured in Ammonia solution with crushed ice. The resulted precipitate was filtered, washed with water three times, and dried under vacuum to get the titled compound **5**.

Yield: 75%. m.p.: 125–127 °C. ^{1}H NMR (400 MHz, $CDCl_3$) δ 10.45 (s, 1H, Ar-H), 8.15 (d, J = 5.2 Hz, 1H, Ar-H), 7.94 (d, J = 7.2 Hz, 2H, Ar-H),

7.45 (m, 4H, Ar-H), 7.36 (t, $J = 8$ Hz, 1H, Ar-H), 7.04 (d, $J = 7.6$ Hz, 1H, Ar-H), 6.98 (d, $J = 8.8$ Hz, 2H, Ar-H), 3.08 (s, 3H, OCH_3). ^{13}C NMR (100 MHz, $CDCl_3$) δ 160.03 (Ar-C), 149.7 (Ar-C), 142.49 (Ar-C), 130.3 (Ar-C), 129.42 (Ar-C), 129.22 (Ar-C), 129.01 (Ar-C), 125.53 (Ar-C), 125.32 (Ar-C), 120.32 (Ar-C), 120.24 (Ar-C), 114.83 (Ar-C), 113.83 (Ar-C), 55.41 (OCH_3).

*5.1.5. N1-(4-(4-(3-methoxyphenyl)-2-phenyl-1H-imidazol-5-yl)pyridin-2-yl)ethane(propan)- diamine **(6–7)***

A solution of compound **5** (2.0 g, 5 mmol) in ethylenediamine (3 mL, 50 mmol, 10 eq.) or propylenediamine (3.7 mL, 50 mmol, 10 eq.) was heated under reflux for 12 h. The reaction mixture was evaporated under vacuum producing the title compounds **6** and **7**, respectively. The produced compounds were subjected to the next step reaction without further purification.

*5.1.6. N-(2-((4-(4-(3-methoxyphenyl)-2-phenyl-1H-imidazol-5-yl) pyridin-2 yl)amino)ethyl(propyl))substituted benzenesulfonamide **(8–9)***

To a solution of compound **6** or **7** (0.3 mmol) in anhydrous dichloromethane (6 mL), DIPEA (0.6 mmol, 2 eq.) was added at 0 °C, stirred for 15 min, then Benzenesulfonyl chlorides (0.36 mmol, 1.2 eq.) was added drop wise. The reaction mixture was stirred at room temperature for 24 h. When the reaction completed, the solvent was removed and the residue was partitioned between ethyl acetate and water. The organic layer was separated and the aqueous layer was extracted with ethyl acetate (3–10 mL). The combined organic layer was washed with brine two times and the organic solvent was evaporated under reduced pressure. The residue was purified by column chromatography (silica gel, hexane-ethyl acetate 2:1 v/v) to give the required products **8** and **9** as solid.

*5.1.6.1. N-(2-((4-(4-(3-methoxyphenyl)-2-phenyl-1H-imidazol-5-yl)pyridin-2-yl)amino)ethyl)benzenesulfonamide **(8a)***. Yield: 65%. m.p.: 139–141 °C. HPLC purity 94.8%, ^1H NMR (400 MHz, $CDCl_3$) δ 7.92 (d, $J = 4.8$ Hz, 2H, Ar-H), 7.73 (d, $J = 5.16$ Hz, 1H, Ar-H), 7.66 (d, $J = 8.16$ Hz, 2H, Ar-H), 7.33 (q, $J = 8.75$ Hz, 5H, Ar-H), 7.19 (t, $J = 7.52$ Hz, 1H, Ar-H), 7 (s, 2H, Ar-H), 6.83 (d, $J = 7.4$ Hz, 1H, Ar-H), 6.66 (s, 1H, Ar-H), 6.6 (d, $J = 3.48$ Hz, 1H, Ar-H), 4.96 (s, 1H, NH), 3.69 (s, 3H, O**C**H_3), 3.3 (s, 2H, **C**$H_2CH_2NHSO_2$), 3.02 (s, 2H, CH_2**C**H_2NHSO_2). ^{13}C NMR (100 MHz, $CDCl_3$) δ 159.62 (Ar-C), 158.48 (Ar-C), 147.05 (Ar-C), 146.59 (Ar-C), 138.85 (Ar-C), 138.43 (Ar-C), 129.66 (Ar-C), 129.55 (Ar-C), 129.27 (Ar-C), 129.03 (Ar-C), 128.79 (Ar-C), 125.73 (Ar-C), 120.99 (Ar-C), 113.95 (Ar-C), 113.85 (Ar-C), 112.24 (Ar-C), 105.92 (Ar-C), 55.25 (O**C**H_3), 44.01 (CH_2**C**H_2NHSO_2), 41.63 (**C**$H_2CH_2NHSO_2$). LC/MS (ESI) 526 (M+1) $^+$.

*5.1.6.2. 4-Chloro-N-(2-((4-(4-(3-methoxyphenyl)-2-phenyl-1H-imidazol-5-yl)pyridin-2-yl)amino)ethyl)benzenesulfonamide **(8b)***. Yield: 60%. m.p.: 130–132 °C. ^1H NMR (400 MHz, $CDCl_3$) δ 7.95 (d, $J = 6.6$ Hz, 2H, Ar-H), 7.79 (d, $J = 5.52$ Hz, 1H, Ar-H), 7.64 (s, 1H, Ar-H), 7.61 (s, 1H, Ar-H), 7.57 (s, 1H, Ar-H), 7.55 (d, $J = 1.72$ Hz, 2H, Ar-H), 7.38 (m, 3H, Ar-H), 7.25 (d, $J = 8$ Hz, 1H, Ar-H), 7.05 (d, $J = 5.92$ Hz, 2H, Ar-H), 6.88 (dd, $J = 1.75$ Hz, 1H, Ar-H), 6.71 (s, 1H, Ar-H), 6.67 (d, $J = 4$ Hz, 1H, Ar-H), 4.94 (s, 1H, NH), 3.75 (s, 3H, O**C**H_3), 3.38 (t, $J = 4.84$ Hz, 2H, C**H**$_2CH_2NHSO_2$), 3.08 (t, $J = 5.32$ Hz, 2H, CH_2C**H**$_2NHSO_2$). ^{13}C NMR (100 MHz, $CDCl_3$) δ 159.73 (Ar-C), 158.41 (Ar-C), 146.89 (Ar-C), 146.43 (Ar-C), 139.03 (Ar-C), 132.25 (Ar-C), 129.79 (Ar-C), 129.51 (Ar-C), 129.12 (Ar-C), 128.87 (Ar-C), 127.34 (Ar-C), 125.63 (Ar-C), 120.93 (Ar-C), 113.93 (Ar-C), 112.26 (Ar-C), 105.95 (Ar-C), 55.32 (O**C**H_3), 44.31 (CH_2**C**H_2NHSO_2), 41.68 (**C**$H_2CH_2NHSO_2$). LC/MS (ESI) 560.4 (M^+).

*5.1.6.3. 4-Bromo-N-(2-((4-(4-(3-methoxyphenyl)-2-phenyl-1H-imidazol-5-yl)pyridin-2-yl)amino)ethyl)benzenesulfonamide **(8c)***. Yield: 71%. m.p.: 127–129 °C. HPLC purity 95.4%, ^1H NMR (400 MHz, $CDCl_3$) δ 7.96 (d, $J = 6.8$ Hz, 2H, Ar-H), 7.79 (m, 3H, Ar-H), 7.39 (m, 3H, Ar-H), 7.25 (d, $J = 8.12$ Hz, 1H, Ar-H), 7.11 (t, $J = 8.48$ Hz, 2H, Ar-H), 7.06 (d, $J = 4$ Hz, 2H, Ar-H), 6.88 (dd, $J = 1.72$ Hz, 1H, Ar-H), 6.73 (s, 1H, Ar-H), 6.66 (d, $J = 4.88$ Hz, 1H, Ar-H), 4.98 (s, 1H, NH), 3.76 (s, 3H, O**C**H_3), 3.39 (d, $J = 4.64$ Hz, 2H, C**H**$_2CH_2NHSO_2$), 3.09 (t, $J = 5.28$ Hz, 2H, CH_2C**H**$_2NHSO_2$). ^{13}C NMR (100 MHz, $CDCl_3$) δ 166.16 (Ar-C), 163.64 (Ar-C), 159.74 (Ar-C), 158.4 (Ar-C), 146.38 (Ar-C), 136.03 (Ar-C), 129.79 (Ar-C), 129.65 (Ar-C), 129.52 (Ar-C), 128.87 (Ar-C), 125.62 (Ar-C), 120.92 (Ar-C), 116.31 (Ar-C), 116.09 (Ar-C), 113.92 (Ar-C), 112.23 (Ar-C), 105.92 (Ar-C), 55.31 (O**C**H_3), 44.21 (CH_2**C**H_2NHSO_2), 41.68 (**C**$H_2CH_2NHSO_2$). LC/MS (ESI) 605.8 (M+1) $^+$.

*5.1.6.4. 4-fluoro-N-(2-((4-(4-(3-methoxyphenyl)-2-phenyl-1H-imidazol-5-yl)pyridin-2-yl)amino)ethyl)benzenesulfonamide **(8d)***. Yield: 65%. m.p.: 133–135 °C. ^1H NMR (400 MHz, $CDCl_3$) δ 7.94 (d, $J = 6.76$ Hz, 2H, Ar-H), 7.79 (t, $J = 1.84$ Hz, 2H, Ar-H), 7.65 (d, $J = 7.84$ Hz, 1H, Ar-H), 7.48 (dd, $J = 0.92$ Hz, 1H, Ar-H), 7.38 (m, 4H, Ar-H), 7.25 (t, $J = 8.12$ Hz, 1H, Ar-H), 7.05 (d, $J = 5.8$ Hz, 2H, Ar-H), 6.87 (dd, $J = 1.76$ Hz, 1H, Ar-H), 6.71 (s, 1H, Ar-H), 6.66 (d, $J = 4.64$ Hz, 1H, Ar-H), 4.93 (s, 1H, NH), 3.74 (s, 3H, O**C**H_3), 3.38 (d, $J = 4.68$ Hz, 2H, C**H**$_2CH_2NHSO_2$), 3.09 (t, $J = 4.96$ Hz, 2H, CH_2C**H**$_2NHSO_2$). ^{13}C NMR (100 MHz, $CDCl_3$) δ 159.71 (Ar-C), 158.44 (Ar-C), 146.45 (Ar-C), 141.76 (Ar-C), 135.11 (Ar-C), 132.54 (Ar-C), 130.35 (Ar-C), 129.76 (Ar-C), 129.51 (Ar-C), 128.86 (Ar-C), 127 (Ar-C), 125.63 (Ar-C), 124.96 (Ar-C), 120.94 (Ar-C), 113.97 (Ar-C), 112.28 (Ar-C), 105.97 (Ar-C), 55.31 (O**C**H_3), 44.4 (CH_2**C**H_2NHSO_2), 41.72 (**C**$H_2CH_2NHSO_2$). LC/MS (ESI) 544.2 (M+1) $^+$.

*5.1.6.5. 3-Chloro-N-(2-((4-(4-(3-methoxyphenyl)-2-phenyl-1H-imidazol-5-yl)pyridin-2-yl)amino)ethyl)benzenesulfonamide **(8e)***. Yield: 74%. m.p.: 120–122 °C. HPLC purity 95.8%, ^1H NMR (400 MHz, $CDCl_3$) δ 7.97 (d, $J = 7.28$ Hz, 2H, Ar-H), 7.82 (d, $J = 5.48$ Hz, 1H, Ar-H), 7.42 (m, 5H, Ar-H), 7.28 (q, $J = 3.2$ Hz, 2H, Ar-H), 7.08 (d, $J = 6.96$ Hz, 2H, Ar-H), 6.9 (t, $J = 1.72$ Hz, 1H, Ar-H), 6.76 (s, 1H, Ar-H), 6.69 (s, 1H, Ar-H), 4.95 (s, 1H, NH), 3.77 (s, 3H, O**C**H_3), 3.47 (q, $J = 5.24$ Hz, 2H, C**H**$_2CH_2NHSO_2$), 3.22 (q, $J = 5.48$ Hz, 2H, CH_2C**H**$_2NHSO_2$). ^{13}C NMR (100 MHz, $CDCl_3$) δ 159.74 (Ar-C), 158.37 (Ar-C), 146.53 (Ar-C), 135.45 (Ar-C), 134.91 (Ar-C), 132.27 (Ar-C), 131.55 (Ar-C), 131.37 (Ar-C), 129.8 (Ar-C), 129.53 (Ar-C), 128.87 (Ar-C), 125.61 (Ar-C), 120.93 (Ar-C), 114.03 (Ar-C), 113.86 (Ar-C), 112.28 (Ar-C), 105.78 (Ar-C), 55.34 (O**C**H_3), 44.3 (CH_2**C**H_2NHSO_2), 41.72 (**C**$H_2CH_2NHSO_2$). LC/MS (ESI) 560.1 (M^+).

*5.1.6.6. 2,6-Dichloro-N-(2-((4-(4-(3-methoxyphenyl)-2-phenyl-1H-imidazol-5-yl)pyridin-2-yl)amino)ethyl)benzenesulfonamide **(8f)***. Yield: 75%. m.p.: 109–111 °C. ^1H NMR (400 MHz, $CDCl_3$) δ 7.92 (d, $J = 6.24$ Hz, 2H, Ar-H), 7.75 (d, $J = 5.52$ Hz, 1H, Ar-H), 7.55 (d, $J = 7.88$ Hz, 1H, Ar-H), 7.47 (dd, $J = 2.04$ Hz, 1H, Ar-H), 7.38 (m, 4H, Ar-H), 7.2 (m, 2H, Ar-H), 7.01 (d, $J = 7.08$ Hz, 2H, Ar-H), 6.84 (t, $J = 1.92$ Hz, 1H, Ar-H), 6.66 (s, 1H, Ar-H), 6.61 (d, $J = 5.08$ Hz, 1H, Ar-H), 4.94 (s, 1H, NH), 3.71 (s, 3H, O**C**H_3), 3.33 (d, $J = 4.48$ Hz, 2H, C**H**$_2CH_2NHSO_2$), 3.06 (t, $J = 5.12$ Hz, 2H, CH_2C**H**$_2NHSO_2$). ^{13}C NMR (100 MHz, $CDCl_3$) δ 163.57 (Ar-C), 161.08 (Ar-C), 159.64 (Ar-C), 158.49 (Ar-C), 146.99 (Ar-C), 142 (Ar-C), 130.88 (Ar-C), 129.69 (Ar-C), 129.06 (Ar-C), 128.82 (Ar-C), 125.68 (Ar-C), 120.96 (Ar-C), 119.53 (Ar-C), 114.36 (Ar-C), 113.9 (Ar-C), 112.26 (Ar-C), 105.96 (Ar-C), 55.26 (O**C**H_3), 44.22 (CH_2**C**H_2NHSO_2), 41.67 (**C**$H_2CH_2NHSO_2$). LC/MS (ESI) 593.9 (M^+).

*5.1.6.7. 3-Fluoro-N-(2-((4-(4-(3-methoxyphenyl)-2-phenyl-1H-imidazol-5-yl)pyridin-2-yl)amino)ethyl)benzenesulfonamide **(8g)***. Yield: 70%. m.p.: 112–114 °C. HPLC purity : 96.3%, ^1H NMR (400 MHz, $CDCl_3$) δ 7.92 (d, $J = 4.8$ Hz, 2H, Ar-H), 7.73 (d, $J = 5.16$ Hz, 1H, Ar-H), 7.66 (d, $J = 8.16$ Hz, 2H, Ar-H), 7.33 (q, $J = 8.75$ Hz, 5H, Ar-H), 7.19 (t, $J = 7.52$ Hz, 1H, Ar-H), 7 (s, 2H, Ar-H), 6.83 (d, $J = 7.4$ Hz, 1H, Ar-H), 6.66 (s, 1H, Ar-H), 6.6 (d, $J = 3.48$ Hz, 1H, Ar-H), 4.96 (s, 1H, NH), 3.69 (s, 3H, O**C**H_3), 3.3 (s, 2H, C**H**$_2CH_2NHSO_2$), 3.02 (s, 2H, CH_2C**H**$_2NHSO_2$). ^{13}C NMR (100 MHz, $CDCl_3$) δ 159.62 (Ar-C), 158.48 (Ar-C), 147.05 (Ar-C), 146.59 (Ar-

C), 138.85 (Ar-C), 138.43 (Ar-C), 129.66 (Ar-C), 129.55 (Ar-C), 129.27 (Ar-C), 129.03 (Ar-C), 128.79 (Ar-C), 125.73 (Ar-C), 120.99 (Ar-C), 113.95 (Ar-C), 113.85 (Ar-C), 112.24 (Ar-C), 105.92 (Ar-C), 55.25 (O**C**H_3), 44.01 (CH_2**C**H_2NHSO_2), 41.63 (**C**$H_2CH_2NHSO_2$). LC/MS (ESI) 544.3 $(M+1)^+$. HRMS calculated for $C_{29}H_{26}FN_5O_3S$ is 543.1740 found: 544.1804 (M+H).

5.1.6.8. N-(2-((4-(4-(3-methoxyphenyl)-2-phenyl-1H-imidazol-5-yl)pyridin-2-yl)amino)ethyl)-4-(trifluoromethyl)benzenesulfonamide ***(8h)***. Yield: 60%. m.p.: 110–112 °C. ^{1}H NMR (400 MHz, $CDCl_3$) δ 7.95 (d, J = 6.6 Hz, 2H, Ar-H), 7.79 (d, J = 5.52 Hz, 1H, Ar-H), 7.64 (s, 1H, Ar-H), 7.61 (s, 1H, Ar-H), 7.57 (s, 1H, Ar-H), 7.55 (d, J = 1.72 Hz, 2H, Ar-H), 7.38 (m, 3H, Ar-H), 7.25 (d, J = 8 Hz, 1H, Ar-H), 7.05 (d, J = 5.92 Hz, 2H, Ar-H), 6.88 (dd, J = 1.75 Hz, 1H, Ar-H), 6.71 (s, 1H, Ar-H), 6.67 (d, J = 4 Hz, 1H, Ar-H), 4.94 (s, 1H, NH), 3.75 (s, 3H, OC**H**$_3$), 3.38 (t, J = 4.84 Hz, 2H, C**H**$_2$CH_2NHSO_2), 3.08 (t, J = 5.32 Hz, 2H, CH_2C**H**$_2$NHSO$_2$). ^{13}C NMR (100 MHz, $CDCl_3$) δ 159.73 (Ar-C), 158.41 (Ar-C), 146.89 (Ar-C), 146.43 (Ar-C), 139.03 (Ar-C), 132.25 (Ar-C), 129.79 (Ar-C), 129.51 (Ar-C), 129.12 (Ar-C), 128.87 (Ar-C), 127.34 (Ar-C), 125.63 (Ar-C), 120.93 (Ar-C), 113.93 (Ar-C), 112.26 (Ar-C), 105.95 (Ar-C), 55.32 (O**C**H_3), 44.31 (CH_2**C**H_2NHSO_2), 41.68 (**C**$H_2CH_2NHSO_2$). LC/MS (ESI) 594.2 $(M+1)^+$.

5.1.6.9. 4-Methoxy-N-(2-((4-(4-(3-methoxyphenyl)-2-phenyl-1H-imidazol-5-yl)pyridin-2-yl)amino)ethyl)benzenesulfonamide ***(8i)***. Yield: 64%. m.p.: 101–103 °C. ^{1}H NMR (400 MHz, $CDCl_3$) δ 7.97 (d, J = 6.8 Hz, 2H, Ar-H), 7.74 (d, J = 5.6 Hz, 1H, Ar-H), 7.69 (d, J = 8.84 Hz, 2H, Ar-H), 7.33 (m, 3H, Ar-H), 7.2 (t, J = 7.8 Hz, 1H, Ar-H), 7.03 (d, J = 7.88 Hz, 2H, Ar-H), 6.87 (d, J = 8.88 Hz, 2H, Ar-H), 6.83 (dd, J = 1.16 Hz, 1H, Ar-H), 6.68 (s, 1H, Ar-H), 6.59 (d, J = 8 Hz, 1H, Ar-H), 5.04 (s, 1H, NH), 3.78 (s, 3H, OC**H**$_3$), 3.71 (s, 3H, OC**H**$_3$), 3.33 (d, J = 4.48 Hz, 2H, C**H**$_2$CH_2NHSO_2), 3.03 (t, J = 5.08 Hz, 2H, CH_2C**H**$_2$NHSO$_2$). ^{13}C NMR (100 MHz, $CDCl_3$) δ 162.75 (Ar-C), 159.59 (Ar-C), 158.52 (Ar-C), 147.04 (Ar-C), 146.65 (Ar-C), 131.32 (Ar-C), 129.63 (Ar-C), 129.01 (Ar-C), 128.94 (Ar-C), 128.77 (Ar-C), 125.74 (Ar-C), 121 (Ar-C), 114.22 (Ar-C), 113.82 (Ar-C), 112.13 (Ar-C), 105.83 (Ar-C), 55.55 (O**C**H_3), 55.25 (O**C**H_3), 43.7 (CH_2**C**H_2NHSO_2), 41.55 (**C**$H_2CH_2NHSO_2$). LC/MS (ESI) 556.3 (M^+).

5.1.6.10. N-(3-((4-(4-(3-methoxyphenyl)-2-phenyl-1H-imidazol-5-yl)pyridin-2-yl)amino)propyl)benzenesulfonamide ***(9a)***. Yield: 65%. m.p.: 105 °C. HPLC purity 96.4%, ^{1}H NMR (400 MHz, $CDCl_3$) δ 7.96 (d, J = 6.76 Hz, 2H, Ar-H), 7.8 (m, 3H, Ar-H), 7.51 (t, J = 4.8 Hz, 1H, Ar-H), 7.43 (t, J = 7.76 Hz, 2H, Ar-H), 7.36 (m, J = 6.8 Hz, 3H, Ar-H), 7.24 (t, J = 8.04 Hz, 1H, Ar-H), 7.05 (d, J = 5.75 Hz, 2H, Ar-H), 6.87 (t, J = 4 Hz, 1H, Ar-H), 6.68 (s, 1H, Ar-H), 6.62 (d, J = 3.72 Hz, 1H, Ar-H), 4.74 (s, 1H, NH), 3.73 (s, 3H, OC**H**$_3$), 3.28 (t, J = 5.92 Hz, 2H, C**H**$_2$C$H_2CH_2NHSO_2$), 2.92 (t, J = 5.76 Hz, 2H, CH_2CH_2C**H**$_2$NHSO$_2$), 1.6 (t, J = 5.8 Hz, 2H, CH_2C**H**$_2CH_2NHSO_2$). ^{13}C NMR (100 MHz, $CDCl_3$) δ 159.66 (Ar-C), 158.77 (Ar-C), 146.9 (Ar-C), 146.69 (Ar-C), 140.08 (Ar-C), 132.41 (Ar-C), 129.59 (Ar-C), 129.03 (Ar-C), 128.83 (Ar-C), 126.86 (Ar-C), 125.68 (Ar-C), 120.95 (Ar-C), 113.96 (Ar-C), 113.82 (Ar-C), 111.73 (Ar-C), 55.29 (O**C**H_3), 40.17 (CH_2CH_2C**H**$_2$NHSO$_2$), 38.37 (**C**$H_2CH_2CH_2NHSO_2$), 29.91 (CH_2**C**$H_2CH_2NHSO_2$). LC/MS (ESI) 540.1 (M^+).

5.1.6.11. 4-Chloro-N-(3-((4-(4-(3-methoxyphenyl)-2-phenyl-1H-imidazol-5-yl)pyridin-2-yl)amino)propyl)benzenesulfonamide ***(9b)***. Yield: 65%. m.p.: 108–110 °C. HPLC purity 97.1% ^{1}H NMR (400 MHz, $CDCl_3$) δ 7.95 (d, J = 6.52 Hz, 2H, Ar-H), 7.82 (d, J = 5.52 Hz, 1H, Ar-H), 7.7 (d, J = 8.64 Hz, 2H, Ar-H), 7.39 (q, J = 6.72 Hz, 4H, Ar-H), 7.29 (d, J = 2.36 Hz, 1H, Ar-H), 7.25 (d, J = 8.04 Hz, 1H, Ar-H), 7.05 (d, J = 6.8 Hz, 2H, Ar-H), 6.89 (t, J = 1.76 Hz, 1H, Ar-H), 6.71 (s, 1H, Ar-H), 6.63 (d, J = 4.76 Hz, 1H, Ar-H), 4.73 (s, 1H, NH), 3.75 (s, 3H, OC**H**$_3$), 3.31 (q, J = 5.64 Hz, 2H, C**H**$_2$C$H_2CH_2NHSO_2$), 2.91 (t, J = 5.68 Hz, 2H, CH_2CH_2C**H**$_2$NHSO$_2$), 1.62 (t, J = 5.8 Hz, 2H, CH_2C**H**$_2CH_2NHSO_2$). ^{13}C NMR (100 MHz, $CDCl_3$) δ 159.7 (Ar-C), 158.71 (Ar-C), 146.87 (Ar-C), 138.73 (Ar-C), 129.77 (Ar-C), 129.54 (Ar-C), 129.26 (Ar-C), 129.08 (Ar-C), 128.85 (Ar-C), 128.36 (Ar-C), 125.65 (Ar-C), 120.93 (Ar-C), 113.92 (Ar-C), 111.74 (Ar-C), 105.81 (Ar-C), 55.3 (O**C**H_3), 40.1 (CH_2CH_2C**H**$_2$NHSO$_2$), 38.34 (**C**$H_2CH_2CH_2NHSO_2$), 29.93 (CH_2**C**$H_2CH_2NHSO_2$). LC/MS (ESI) 574.1 (M^+).

5.1.6.12. 4-Bromo-N-(3-((4-(4-(3-methoxyphenyl)-2-phenyl-1H-imidazol-5-yl)pyridin-2-yl)amino)propyl)benzenesulfonamide ***(9c)***. Yield: 70%. m.p.: 120–122 °C. HPLC purity 96.8% ^{1}H NMR (400 MHz, $CDCl_3$) δ 7.96 (d, J = 6.72 Hz, 2H, Ar-H), 7.82 (d, J = 5.56 Hz, 1H, Ar-H), 7.64 (d, J = 8.6 Hz, 2H, Ar-H), 7.57 (d, J = 8.6 Hz, 2H, Ar-H), 7.4 (d, J = 7.4 Hz, 2H, Ar-H), 7.29 (q, J = 5.16 Hz, 2H, Ar-H), 7.06 (d, J = 7.24 Hz, 2H, Ar-H), 6.91 (t, J = 1.76 Hz, 1H, Ar-H), 6.74 (s, 1H, Ar-H), 6.66 (d, J = 4.96 Hz, 1H, Ar-H), 4.84 (s, 1H, NH), 3.76 (s, 3H, OC**H**$_3$), 3.33 (q, J = 5.8 Hz, 2H, C**H**$_2$C$H_2CH_2NHSO_2$), 2.93 (t, J = 5.6 Hz, 2H, CH_2CH_2C**H**$_2$NHSO$_2$), 1.64 (m, 2H, CH_2C**H**$_2CH_2NHSO_2$). ^{13}C NMR (100 MHz, $CDCl_3$) δ 159.74 (Ar-C), 158.57 (Ar-C), 139.31 (Ar-C), 132.24 (Ar-C), 129.83 (Ar-C), 129.51 (Ar-C), 129.12 (Ar-C), 128.88 (Ar-C), 128.48 (Ar-C), 127.2 (Ar-C), 125.63 (Ar-C), 120.92 (Ar-C), 114.03 (Ar-C), 113.93 (Ar-C), 111.71 (Ar-C), 55.33 (O**C**H_3), 40.09 (CH_2CH_2C**H**$_2$NHSO$_2$), 38.35 (**C**$H_2CH_2CH_2NHSO_2$), 29.93 (CH_2**C**$H_2CH_2NHSO_2$). LC/MS (ESI) 618.1 (M^+).

5.1.6.13. 4-Fluoro-N-(3-((4-(4-(3-methoxyphenyl)-2-phenyl-1H-imidazol-5-yl)pyridin-2-yl)amino)propyl)benzenesulfonamide ***(9d)***. Yield: 72%. m.p.: 112–114 °C. HPLC purity 97.4%, ^{1}H NMR (400 MHz, $CDCl_3$) δ 7.94 (t, J = 1.8 Hz, 2H, Ar-H), 7.77 (m, 3H, Ar-H), 7.35 (d, J = 6.76 Hz, 3H, Ar-H), 7.22 (t, J = 8.04 Hz, 1H, Ar-H), 7.08 (t, J = 8.56 Hz, 1H, Ar-H), 7.02 (d, J = 5.68 Hz, 2H, Ar-H), 6.86 (t, J = 1.84 Hz, 1H, Ar-H), 6.67 (s, 1H, Ar-H), 6.59 (d, J = 5.04 Hz, 1H, Ar-H), 4.7 (s, 1H, NH), 3.71 (s, 3H, OC**H**$_3$), 3.25 (d, J = 8 Hz, 2H, C**H**$_2$C$H_2CH_2NHSO_2$), 2.88 (t, J = 5.64 Hz, 2H, CH_2CH_2C**H**$_2$NHSO$_2$), 1.58 (t, J = 8 Hz, 2H, CH_2C**H**$_2CH_2NHSO_2$). ^{13}C NMR (100 MHz, $CDCl_3$) δ 166.08 (Ar-C), 163.55 (Ar-C), 159.63 (Ar-C), 158.84 (Ar-C), 146.96 (Ar-C), 146.72 (Ar-C), 136.2 (Ar-C), 129.69 (Ar-C), 129.03 (Ar-C), 128.81 (Ar-C), 125.71 (Ar-C), 120.96 (Ar-C), 116.07 (Ar-C), 113.91 (Ar-C), 111.77 (Ar-C), 105.75 (Ar-C), 55.25 (O**C**H_3), 40.12 (CH_2CH_2C**H**$_2$NHSO$_2$), 38.33 (**C**$H_2CH_2CH_2NHSO_2$), 29.86 (CH_2**C**$H_2CH_2NHSO_2$). 19F NMR (400 MHz, DMSO-d_6) −107.17 (d, 1F, J = 8.00 Hz). LC/MS (ESI) 558.1 (M^+).

5.1.6.14. 3-Chloro-N-(3-((4-(4-(3-methoxyphenyl)-2-phenyl-1H-imidazol-5-yl)pyridin-2-yl)amino)propyl)benzenesulfonamide ***(9e)***. Yield: 71%. m.p.: 113–115 °C. HPLC 97.3%, ^{1}H NMR (400 MHz, $CDCl_3$) δ 7.94 (t, J = 1.36 Hz, 2H, Ar-H), 7.78 (m, 2H, Ar-H), 7.64 (d, J = 7.8 Hz, 1H, Ar-H), 7.47 (q, J = 0.8 Hz, 1H, Ar-H), 7.35 (m, 4H, Ar-H), 7.22 (t, J = 8.04 Hz, 1H, Ar-H), 7.02 (d, J = 6.12 Hz, 2H, Ar-H), 6.86 (t, J = 1.8 Hz, 1H, Ar-H), 6.67 (s, 1H, Ar-H), 6.61 (d, J = 5.04 Hz, 1H, Ar-H), 4.71 (s, 1H, NH), 3.71 (s, 3H, OC**H**$_3$), 3.27 (d, J = 5.76 Hz, 2H, C**H**$_2$C$H_2CH_2NHSO_2$), 2.9 (t, J = 5.6 Hz, 2H, CH_2CH_2C**H**$_2$NHSO$_2$), 1.59 (t, J = 5.72 Hz, 2H, CH_2C**H**$_2CH_2NHSO_2$). ^{13}C NMR (100 MHz, $CDCl_3$) δ 159.63 (Ar-C), 158.81 (Ar-C), 146.67 (Ar-C), 141.98 (Ar-C), 135.1 (Ar-C), 132.46 (Ar-C), 130.36 (Ar-C), 129.55 (Ar-C), 128.83 (Ar-C), 126.95 (Ar-C), 125.69 (Ar-C), 124.93 (Ar-C), 120.97 (Ar-C), 113.89 (Ar-C), 111.77 (Ar-C), 105.79 (Ar-C), 55.27 (O**C**H_3), 40.14 (CH_2CH_2C**H**$_2$NHSO$_2$), 38.32 (**C**$H_2CH_2CH_2NHSO_2$), 29.94 (CH_2**C**$H_2CH_2NHSO_2$). LC/MS (ESI) 574.1 $(M+1)^+$. HRMS calculated for $C_{30}H_{28}ClN_5O_3S$ is 573.1601 found : 574.1689 (M+H).

5.1.6.15. 2,6-dichloro-N-(3-((4-(4-(3-methoxyphenyl)-2-phenyl-1H-imidazol-5-yl)pyridin-2-yl)amino)propyl)benzenesulfonamide ***(9f)***. Yield: 63%. m.p.: 117–119 °C. HPLC purity 95.8%, ^{1}H NMR (400 MHz, $CDCl_3$) δ 7.94 (d, J = 6.84 Hz, 2H, Ar-H), 7.82 (d, J = 5.36 Hz, 1H, Ar-H), 7.41 (d, J = 7.88 Hz, 2H, Ar-H), 7.35 (d, J = 7.52 Hz, 2H, Ar-H), 7.26 (m, 3H, Ar-H), 7.02 (s, 2H, Ar-H), 6.84 (d, J = 7.56 Hz, 1H, Ar-H), 6.63 (d, J =

15.2 Hz, 2H, Ar-H), 4.66 (s, 1H, NH), 3.71 (s, 3H, OC**H**$_3$), 3.3 (d, J = 5.44 Hz, 2H, C**H**$_2$CH$_2$CH$_2$NHSO$_2$), 3.04 (d, J = 4.6 Hz, 2H, CH$_2$CH$_2$C**H**$_2$NHSO$_2$), 1.59 (d, J = 5.04 Hz, 2H, CH$_2$C**H**$_2$CH$_2$NHSO$_2$). ^{13}C NMR (100 MHz, CDCl$_3$) δ 159.6 (Ar-C), 158.92 (Ar-C), 147.05 (Ar-C), 144.68 (Ar-C), 135.97 (Ar-C), 134.76 (Ar-C), 132.23 (Ar-C), 131.39 (Ar-C), 129.63 (Ar-C), 128.79 (Ar-C), 125.71 (Ar-C), 120.98 (Ar-C), 117.23 (Ar-C), 113.96 (Ar-C), 111.81 (Ar-C), 105.69 (Ar-C), 55.27 (O**C**H$_3$), 40.22 (CH$_2$CH$_2$**C**H$_2$NHSO$_2$), 38.31 (**C**H$_2$CH$_2$CH$_2$NHSO$_2$), 30.29 (CH$_2$**C**H$_2$CH$_2$NHSO$_2$). LC/MS (ESI) 608.54 (M$^+$).

5.1.6.16. 3-fluoro-N-(3-((4-(4-(3-methoxyphenyl)-2-phenyl-1H-imidazol-5-yl)pyridin-2-yl)amino)propyl)benzenesulfonamide ***(9g)***. Yield: 72%. m.p.: 101–103 °C. ^{1}H NMR (400 MHz, CDCl$_3$) δ 7.94 (d, J = 6.56 Hz, 2H, Ar-H), 7.82 (d, J = 5.52 Hz, 1H, Ar-H), 7.57 (d, J = 7.88 Hz, 1H, Ar-H), 7.5 (m, 1H, Ar-H), 7.4 (m, 4H, Ar-H), 7.23 (t, J = 8.28 Hz, 1H, Ar-H), 7.2 (dd, J = 1.92 Hz, 1H, Ar-H), 7.04 (d, J = 6.84 Hz, 2H, Ar-H), 6.88 (t, J = 1.96 Hz, 1H, Ar-H), 6.71 (s, 1H, Ar-H), 6.63 (d, J = 5.2 Hz, 1H, Ar-H), 4.72 (s, 1H, NH), 3.74 (s, 3H, OC**H**$_3$), 3.3 (q, J = 5.88 Hz, 2H, C**H**$_2$CH$_2$CH$_2$NHSO$_2$), 2.93 (t, J = 5.88 Hz, 2H, CH$_2$CH$_2$C**H**$_2$NHSO$_2$), 1.62 (t, J = 5.92 Hz, 2H, CH$_2$C**H**$_2$CH$_2$NHSO$_2$). ^{13}C NMR (100 MHz, CDCl$_3$) δ 161.1 (Ar-C), 159.68 (Ar-C), 158.74 (Ar-C), 146.87 (Ar-C), 142.33 (Ar-C), 130.86 (Ar-C), 130.79 (Ar-C), 129.53 (Ar-C), 128.85 (Ar-C), 125.64 (Ar-C), 122.62 (Ar-C), 120.94 (Ar-C), 119.4 (Ar-C), 114.36 (Ar-C), 113.87 (Ar-C), 111.75 (Ar-C), 55.29 (O**C**H$_3$), 40.13 (CH$_2$CH$_2$**C**H$_2$NHSO$_2$), 38.31 (**C**H$_2$CH$_2$CH$_2$NHSO$_2$), 29.98 (CH$_2$**C**H$_2$CH$_2$NHSO$_2$). LC/MS (ESI) 557.64 (M$^+$).

5.1.6.17. N-(3-((4-(4-(3-methoxyphenyl)-2-phenyl-1H-imidazol-5-yl)pyridin-2-yl)amino)propyl)-4-(trifluoromethyl)benzenesulfonamide ***(9h)***. Yield: 65%. m.p.: 110–112 °C.HPLC purity 96.2%, ^{1}H NMR (400 MHz, CDCl$_3$) δ 7.92 (t, J = 2.16 Hz, 2H, Ar-H), 7.88 (d, J = 8 Hz, 2H, Ar-H), 7.68 (d, J = 8.32 Hz, 2H, Ar-H), 7.34 (t, J = 1.36 Hz, 3H, Ar-H), 7.23 (t, J = 8.08 Hz, 1H, Ar-H), 7.01 (d, J = 6.08 Hz, 2H, Ar-H), 6.86 (t, J = 4 Hz, 1H, Ar-H), 6.7 (s, 1H, Ar-H), 6.6 (d, J = 5.16 Hz, 1H, Ar-H), 4.68 (s, 1H, NH), 3.71 (s, 3H, OC**H**$_3$), 3.27 (d, J = 4 Hz, 2H, C**H**$_2$CH$_2$CH$_2$NHSO$_2$), 2.92 (t, J = 4.08 Hz, 2H, CH$_2$CH$_2$C**H**$_2$NHSO$_2$), 1.59 (t, J = 5.08 Hz, 2H, CH$_2$C**H**$_2$CH$_2$NHSO$_2$). ^{13}C NMR (100 MHz, CDCl$_3$) δ 159.66 (Ar-C), 158.85 (Ar-C), 146.94 (Ar-C), 143.95 (Ar-C), 134.1 (Ar-C), 129.72 (Ar-C), 128.82 (Ar-C), 127.35 (Ar-C), 126.16 (Ar-C), 125.69 (Ar-C), 124.61 (Ar-C), 121.9 (Ar-C), 120.95 (Ar-C), 113.97 (Ar-C), 111.81 (Ar-C), 105.88 (Ar-C), 55.24 (O**C**H$_3$), 40.12 (CH$_2$CH$_2$**C**H$_2$NHSO$_2$), 38.31 (**C**H$_2$CH$_2$CH$_2$NHSO$_2$), 29.98 (CH$_2$**C**H$_2$CH$_2$NHSO$_2$). LC/MS (ESI) 607.65 (M$^+$).

5.1.6.18. 4-methoxy-N-(3-((4-(4-(3-methoxyphenyl)-2-phenyl-1H-imidazol-5-yl)pyridin-2-yl)amino)propyl)benzenesulfonamide ***(9i)***. Yield: 60%. m.p.: 100–102 °C. HPLC purity 95.9%, ^{1}H NMR (400 MHz, CDCl$_3$) δ 7.97 (d, J = 6.84 Hz, 2H, Ar-H), 7.81 (d, J = 5.52 Hz, 1H, Ar-H), 7.36 (q, J = 6.12 Hz, 3H, Ar-H), 7.23 (t, J = 8.08 Hz, 1H, Ar-H), 7.06 (d, J = 5.2 Hz, 2H, Ar-H), 6.87 (m, 3H, Ar-H), 6.67 (s, 1H, Ar-H), 6.61 (s, 1H, Ar-H), 4.76 (s, 1H, NH), 3.81 (s, 3H, OC**H**$_3$), 3.72 (s, 3H, OC**H**$_3$), 3.27 (q, J = 5.84 Hz, 2H, C**H**$_2$CH$_2$CH$_2$NHSO$_2$), 2.88 (t, J = 5.4 Hz, 2H, CH$_2$CH$_2$C**H**$_2$NHSO$_2$), 1.6 (t, J = 5.88 Hz, 2H, CH$_2$C**H**$_2$CH$_2$NHSO$_2$). ^{13}C NMR (100 MHz, CDCl$_3$) δ 162.69 (Ar-C), 159.63 (Ar-C), 158.8 (Ar-C), 146.79 (Ar-C), 129.63 (Ar-C), 129.02 (Ar-C), 128.8 (Ar-C), 125.71 (Ar-C), 120.97 (Ar-C), 114.19 (Ar-C), 113.95 (Ar-C), 113.79 (Ar-C), 111.74 (Ar-C), 55.55 (O**C**H$_3$), 55.27 (O**C**H3), 40.19 (CH$_2$CH$_2$**C**H$_2$NHSO$_2$), 38.45 (**C**H$_2$CH$_2$CH$_2$NHSO$_2$), 29.77 (CH$_2$**C**H$_2$CH$_2$NHSO$_2$). LC/MS (ESI) 570.3 (M$^+$).

5.1.7. N-(2-((4-(4-(3-hydroxyphenyl)-2-phenyl-1H-imidazol-5-yl)pyridin-2 yl)amino)ethyl(propyl))substituted benzenesulfonamide ***(10–11)***

To a solution of compound **8** or **9** (0.3 mmol) in methylene chloride (3 mL), BBr$_3$ (3 mL of a 1 M solution in methylene chloride) was added drop wise at −78 °C under N$_2$. The reaction mixture was stirred at the same temperature for 1 h, and then allowed to warm to room temperature and stirred for another 3 h. The mixture was quenched with saturated aqueous Na$_2$CO$_3$. Ethyl acetate (5 mL) was added and the organic layer was separated. The aqueous layer was extracted with ethyl acetate (X 2). The combined organic layer extracts were washed with brine, and dried over anhydrous Na$_2$SO$_4$. After evaporation of the organic solvent, the residue was purified by short column chromatography (silica gel, using ethyl acetate then switching to ethyl acetate–methanol 4:1 v/v) to yield the title compound.

5.1.7.1. N-(2-((4-(4-(3-hydroxyphenyl)-2-phenyl-1H-imidazol-5-yl)pyridin-2-yl)amino)ethyl)benzenesulfonamide ***(10a)***. Yield: 68%. m.p.: 180–182 °C. HPLC purity 97.2% ^{1}H NMR (400 MHz, MeOH) δ 7.98 (d, J = 7.2 Hz, 2H, Ar-H), 7.82 (q, J = 1.6 Hz, 3H, Ar-H), 7.51 (m, 1H, Ar-H), 7.46 (m, 4H, Ar-H), 7.39 (t, J = 2.4 Hz, 1H, Ar-H), 7.23 (t, J = 8 Hz, 1H, Ar-H), 6.98 (t, J = 2.4 Hz, 1H, Ar-H), 6.83 (dd, J = 2.4 Hz, 1H, Ar-H), 6.7 (d, J = 5.2 Hz, 2H, Ar-H), 3.32 (q, J = 4 Hz, 2H, C**H**$_2$CH$_2$NHSO$_2$), 3.03 (t, J = 6 Hz, 2H, CH$_2$C**H**$_2$NHSO$_2$). ^{13}C NMR (100 MHz, MeOD) δ 158.69 (Ar-C), 157.37 (Ar-C), 147.18 (Ar-C), 146.43 (Ar-C), 140.25 (Ar-C), 132.28 (Ar-C), 129.63 (Ar-C), 129.58 (Ar-C), 128.86 (Ar-C), 128.58 (Ar-C), 126.57 (Ar-C), 125.7 (Ar-C), 119.8 (Ar-C), 115.43 (Ar-C), 115 (Ar-C), 111.48 (Ar-C), 106.22 (Ar-C), 42.35 (CH$_2$**C**H$_2$NHSO$_2$), 41.06 (**C**H$_2$CH$_2$NHSO$_2$). LC/MS (ESI) 512.0 (M$^+$).

5.1.7.2. 4-chloro-N-(2-((4-(4-(3-hydroxyphenyl)-2-phenyl-1H-imidazol-5-yl)pyridin-2-yl)amino)ethyl)benzenesulfonamide ***(10b)***. Yield: 74%. m.p.: 115–117 °C. HPLC purity 97.1%^{1}H NMR (400 MHz, MeOD) δ 8.01 (t, J = 1.2 Hz, 2H, Ar-H), 7.8 (t, J = 6.44 Hz, 3H, Ar-H), 4.89 (m, 4H, Ar-H), 7.4 (t, J = 7.28 Hz, 1H, Ar-H), 7.25 (m, 1H, Ar-H), 7 (q, J = 1.84 Hz, 2H, Ar-H), 6.85 (dd, J = 1.36 Hz, 1H, Ar-H), 6.71 (t, J = 5.68 Hz, 2H, Ar-H), 3.33 (t, J = 8 Hz, 2H, C**H**$_2$CH$_2$NHSO$_2$), 3.07 (t, J = 5.88 Hz, 2H, CH$_2$C**H**$_2$NHSO$_2$). ^{13}C NMR (100 MHz, MeOD) δ 158.62 (Ar-C), 157.36 (Ar-C), 147.17 (Ar-C), 146.41 (Ar-C), 139.1 (Ar-C), 138.38 (Ar-C), 129.64 (Ar-C), 129.58 (Ar-C), 129.04 (Ar-C), 128.82 (Ar-C), 128.59 (Ar-C), 128.3 (Ar-C), 125.72 (Ar-C), 119.85 (Ar-C), 115.48 (Ar-C), 115.03 (Ar-C), 111.45 (Ar-C), 106.14 (Ar-C), 42.39 (CH$_2$**C**H$_2$NHSO$_2$), 40.98 (**C**H$_2$CH$_2$NHSO$_2$). LC/MS (ESI) 546.3 (M$^+$).

5.1.7.3. 4-bromo-N-(2-((4-(4-(3-hydroxyphenyl)-2-phenyl-1H-imidazol-5-yl)pyridin-2-yl)amino)ethyl)benzenesulfonamide ***(10c)***. Yield: 72%. m.p.: 145–147 °C. HPLC purity 97.6%, ^{1}H NMR (400 MHz, MeOD) δ 8 (d, J = 1.2 Hz, 1H, Ar-H), 7.98 (s, 1H, Ar-H), 7.82 (d, J = 5.52 Hz, 1H, Ar-H), 7.71 (s, 1H, Ar-H), 7.69 (s, 1H, Ar-H), 7.64 (d, J = 8 Hz, 2H, Ar-H), 7.45 (m, 3H, Ar-H), 7.25 (t, J = 8 Hz, 1H, Ar-H), 6.98 (t, J = 1.2 Hz, 2H, Ar-H), 6.83 (m, 1H, Ar-H), 6.72 (dd, J = 1.08 Hz, 1H, Ar-H), 6.67 (s, 1H, Ar-H), 3.33 (q, J = 1.64 Hz, 2H, C**H**$_2$CH$_2$NHSO$_2$), 3.06 (t, J = 5.96 Hz, 2H, CH$_2$C**H**$_2$NHSO$_2$). ^{13}C NMR (100 MHz, MeOD) δ 158.61 (Ar-C), 157.36 (Ar-C), 147.16 (Ar-C), 146.44 (Ar-C), 139.63 (Ar-C), 132.03 (Ar-C), 129.65 (Ar-C), 129.55 (Ar-C), 128.78 (Ar-C), 128.55 (Ar-C), 128.33 (Ar-C), 126.73 (Ar-C), 125.7 (Ar-C), 119.82 (Ar-C), 115.45 (Ar-C), 114.98 (Ar-C), 111.42 (Ar-C), 106.11 (Ar-C), 42.33 (CH$_2$**C**H$_2$NHSO$_2$), 40.94 (**C**H$_2$CH$_2$NHSO$_2$). HRMS calculated for C$_{28}$H$_{24}$BrN$_5$O$_3$S is 590.9460 found: 591.5048 (M+H).

5.1.7.4. 4-fluoro-N-(2-((4-(4-(3-hydroxyphenyl)-2-phenyl-1H-imidazol-5-yl)pyridin-2-yl)amino)ethyl)benzenesulfonamide ***(10d)***. Yield: 74%. m.p.: 143–145 °C. HPLC purity 97.8 %^{1}H NMR (400 MHz, MeOD) δ 7.99 (d, J = 7.2 Hz, 2H, Ar-H), 7.87 (m, 2H, Ar-H), 7.82 (d, J = 4 Hz, 1H, Ar-H), 7.47 (t, J = 7.08 Hz, 2H, Ar-H), 7.41 (t, J = 7.24 Hz, 1H, Ar-H), 7.23 (m, 3H, Ar-H), 7.98 (t, J = 6.48 Hz, 2H, Ar-H), 6.83 (m, 1H, Ar-H), 6.71 (t, J = 3.72 Hz, 2H, Ar-H), 3.33 (t, J = 6 Hz, 2H, C**H**$_2$CH$_2$NHSO$_2$), 3.05 (t, J = 6 Hz, 2H, CH$_2$C**H**$_2$NHSO$_2$). ^{13}C NMR (100 MHz, MeOD) δ 166.16 (Ar-C), 163.65 (Ar-C), 158.66 (Ar-C), 157.35 (Ar-C), 147.17 (Ar-C), 146.42 (Ar-C), 136.56 (Ar-C), 129.63 (Ar-C), 129.45 (Ar-C), 128.78 (Ar-C), 128.55 (Ar-C), 125.69 (Ar-C), 119.81 (Ar-C), 115.92 (Ar-C), 115.43

(Ar-C), 114.98 (Ar-C), 111.45 (Ar-C), 106.15 (Ar-C), 42.31 ($CH_2\mathbf{C}H_2NHSO_2$), 41 ($\mathbf{C}H_2CH_2NHSO_2$). LC/MS 530 (M^+). HRMS calculated for $C_{28}H_{24}FN_5O_3S$ is 529.5904 found : 530.1628 (M+H).

*5.1.7.5. 3-chloro-N-(2-((4-(4-(3-hydroxyphenyl)-2-phenyl-1H-imidazol-5-yl)pyridin-2-yl)amino)ethyl)benzenesulfonamide **(10e)***. Yield: 73%. m.p.: 138–140 °C. ^{1}H NMR (400 MHz, MeOD) δ 7.98 (d, J = 7.2 Hz, 2H, Ar-H), 7.83 (q, J = 2.04 Hz, 2H, Ar-H), 7.73 (d, J = 7.76 Hz, 1H, Ar-H), 7.53 (dd, J = 0.76 Hz, 1H, Ar-H), 7.46 (m, 3H, Ar-H), 7.39 (t, J = 7.24 Hz, 1H, Ar-H), 7.24 (m, 1H, Ar-H), 6.99 (t, J = 2.24 Hz, 2H, Ar-H), 6.84 (dd, J = 1.48 Hz, 1H, Ar-H), 6.71 (t, J = 5.56 Hz, 2H, Ar-H), 3.33 (t, J = 5.92 Hz, 2H, $C\mathbf{H}_2CH_2NHSO_2$), 3.06 (t, J = 5.96 Hz, 2H, $CH_2C\mathbf{H}_2NHSO_2$). ^{13}C NMR (100 MHz, MeOD) δ 158.65 (Ar-C), 157.35 (Ar-C), 147.16 (Ar-C), 146.48 (Ar-C), 142.28 (Ar-C), 134.73 (Ar-C), 132.2 (Ar-C), 130.46 (Ar-C), 129.55 (Ar-C), 128.56 (Ar-C), 126.48 (Ar-C), 125.69 (Ar-C), 124.93 (Ar-C), 119.84 (Ar-C), 115.46 (Ar-C), 115 (Ar-C), 111.48 (Ar-C), 106.13 (Ar-C), 42.37 ($CH_2\mathbf{C}H_2NHSO_2$), 41.02 ($\mathbf{C}H_2CH_2NHSO_2$). LC/MS (ESI) 545.8 (M^+).

*5.1.7.6. 2,6-dichloro-N-(2-((4-(4-(3-hydroxyphenyl)-2-phenyl-1H-imidazol-5-yl)pyridin-2-yl)amino)ethyl)benzenesulfonamide **(10f)***. Yield: 64%. m.p.: 141–143 °C. ^{1}H NMR (400 MHz, MeOD) δ 7.98 (d, J = 7.6 Hz, 2H, Ar-H), 7.78 (d, J = 5.6 Hz, 1H, Ar-H), 7.41 (m, 5H, Ar-H), 7.27 (m, 2H, Ar-H), 6.98 (t, J = 6.8 Hz, 2H, Ar-H), 6.83 (dd, J = 2 Hz, 1H, Ar-H), 6.7 (d, J = 5.6 Hz, 1H, Ar-H), 6.65 (s, 1H, Ar-H), 3.33 (q, J = 5.6 Hz, 2H, $C\mathbf{H}_2CH_2NHSO_2$), 3.18 (t, J = 6 Hz, 2H, $CH_2C\mathbf{H}_2NHSO_2$). ^{13}C NMR (100 MHz, MeOD) δ 158.58 (Ar-C), 157.37 (Ar-C), 147.16 (Ar-C), 146.44 (Ar-C), 135.55 (Ar-C), 134.45 (Ar-C), 132.47 (Ar-C), 131.28 (Ar-C), 129.63 (Ar-C), 128.81 (Ar-C), 128.59 (Ar-C), 125.7 (Ar-C), 119.85 (Ar-C), 115.47 (Ar-C), 115 (Ar-C), 111.51 (Ar-C), 106.24 (Ar-C), 42.34 ($CH_2\mathbf{C}H_2NHSO_2$), 40.9 ($\mathbf{C}H_2CH_2NHSO_2$). LC/MS (ESI) 579.9 (M^+).

*5.1.7.7. 3-fluoro-N-(2-((4-(4-(3-hydroxyphenyl)-2-phenyl-1H-imidazol-5-yl)pyridin-2-yl)amino)ethyl)benzenesulfonamide **(10g)***. Yield: 74%. m.p.: 118–120 °C. ^{1}H NMR (400 MHz, MeOD) δ 8 (d, J = 7.32 Hz, 2H, Ar-H), 7.82 (d, J = 6.04 Hz, 1H, Ar-H), 7.66 (d, J = 8 Hz, 1H, Ar-H), 7.58 (d, J = 8.24 Hz, 1H, Ar-H), 7.53 (t, J = 8.08 Hz, 1H, Ar-H), 7.46 (m, 2H, Ar-H), 7.39 (t, J = 7.16 Hz, 1H, Ar-H), 7.28 (m, 2H, Ar-H), 6.99 (d, J = 6.88 Hz, 2H, Ar-H), 6.85 (t, J = 1.68 Hz, 1H, Ar-H), 6.72 (d, J = 4.64 Hz, 2H, Ar-H), 3.35 (t, J = 5.92 Hz, 2H, $C\mathbf{H}_2CH_2NHSO_2$), 3.08 (t, J = 6 Hz, 2H, $CH_2C\mathbf{H}_2NHSO_2$). ^{13}C NMR (100 MHz, MeOD) δ 163.65 (Ar-C), 161.17 (Ar-C), 158.58 (Ar-C), 147.18 (Ar-C), 146.26 (Ar-C), 142.58 (Ar-C), 142.51 (Ar-C), 131.05 (Ar-C), 130.98 (Ar-C), 129.67 (Ar-C), 128.67 (Ar-C), 125.72 (Ar-C), 122.57 (Ar-C), 119.86 (Ar-C), 115.48 (Ar-C), 113.81 (Ar-C), 111.49 (Ar-C), 104.19 (Ar-C), 42.41 ($CH_2\mathbf{C}H_2NHSO_2$), 41.05 ($\mathbf{C}H_2CH_2NHSO_2$). LC/MS (ESI) 530.1 (M^+).

*5.1.7.8. N-(2-((4-(4-(3-hydroxyphenyl)-2-phenyl-1H-imidazol-5-yl)pyridin-2-yl)amino)ethyl)-4-(trifluoromethyl)benzenesulfonamide **(10h)***. Yield: 65%. m.p.: 117–119 °C. ^{1}H NMR (400 MHz, MeOD) δ 8 (q, J = 2.16 Hz, 4H, Ar-H), 7.81 (d, J = 7.92 Hz, 3H, Ar-H), 7.46 (t, J = 7.68 Hz, 2H, Ar-H), 7.39 (m, 1H, Ar-H), 7.24 (t, J = 8.08 Hz, 1H, Ar-H), 6.99 (m, J = 2.08 Hz, 2H, Ar-H), 6.84 (dd, J = 1.44 Hz, 1H, Ar-H), 6.71 (t, J = 4 Hz, 2H, Ar-H), 3.33 (m, 2H, $C\mathbf{H}_2CH_2NHSO_2$), 3.1 (t, J = 5.92 Hz, 2H, $CH_2C\mathbf{H}_2NHSO_2$). ^{13}C NMR (100 MHz, MeOD) δ 158.65 (Ar-C), 157.34 (Ar-C), 147.19 (Ar-C), 146.48 (Ar-C), 144.34 (Ar-C), 133.63 (Ar-C), 133.3 (Ar-C), 129.62 (Ar-C), 128.55 (Ar-C), 127.37 (Ar-C), 125.98 (Ar-C), 124.86 (Ar-C), 122.15 (Ar-C), 119.84 (Ar-C), 115.46 (Ar-C), 115 (Ar-C), 111.51 (Ar-C), 106.13 (Ar-C), 42.41 ($CH_2\mathbf{C}H_2NHSO_2$), 41.07 ($\mathbf{C}H_2CH_2NHSO_2$). 19F NMR (400 MHz, DMSO-d_6) −16.55 (s, 1F). LC/MS (ESI) 580.1 (M^+).

*5.1.7.9. N-(2-((4-(4-(3-hydroxyphenyl)-2-phenyl-1H-imidazol-5-yl)pyridin-2-yl)amino)ethyl)-4-methoxybenzenesulfonamide **(10i)***. Yield: 55%. m.p.: 120–122 °C. HPLC purity 96.4%, ^{1}H NMR (400 MHz, MeOD) δ 7.99 (d, J = 7.36 Hz, 2H, Ar-H), 7.82 (d, J = 5.48 Hz, 1H, Ar-H), 7.75 (d, J = 8.8 Hz, 2H, Ar-H), 7.48 (t, J = 8.76 Hz, 2H, Ar-H), 7.42 (t, J = 7.36 Hz, 1H, Ar-H), 7.25 (t, J = 8.16 Hz, 1H, Ar-H), 6.98 (t, J = 6.64 Hz, 4H, Ar-H), 6.85 (dd, J = 5.36 Hz, 1H, Ar-H), 6.7 (t, J = 5.64 Hz, 2H, Ar-H), 3.7 (s, 3H, $C\mathbf{H}_3$), 3.32 (t, J = 6.56 Hz, 2H, $C\mathbf{H}_2CH_2NHSO_2$), 3.02 (t, J = 6 Hz, 2H, $CH_2C\mathbf{H}_2NHSO_2$). ^{13}C NMR (100 MHz, MeOD) δ 162.92 (Ar-C), 158.68 (Ar-C), 157.36 (Ar-C), 147.15 (Ar-C), 146.42 (Ar-C), 131.66 (Ar-C), 129.54 (Ar-C), 128.78 (Ar-C), 128.55 (Ar-C), 125.68 (Ar-C), 119.8 (Ar-C), 115.42 (Ar-C), 115.26 (Ar-C), 114.96 (Ar-C), 113.9 (Ar-C), 111.37 (Ar-C), 106.11 (Ar-C), 54.75 ($\mathbf{C}H_3$), 42.26 ($CH_2\mathbf{C}H_2NHSO_2$), 40.92 ($\mathbf{C}H_2CH_2NHSO_2$). LC/MS (ESI) 542 (M^+).

*5.1.7.10. 4-hydroxy-N-(2-((4-(4-(3-hydroxyphenyl)-2-phenyl-1H-imidazol-5-yl)pyridin-2-yl)amino)ethyl)benzenesulfonamide **(10j)***. Yield: 55%. m.p.: 122–124 °C. HPLC purity 95.8% ^{1}H NMR (400 MHz, MeOD) δ 8 (d, J = 8.4 Hz, 1H, Ar-H), 7.69 (d, J = 8.8 Hz, 1H, Ar-H), 7.48 (t, J = 6.8 Hz, 1H, Ar-H), 7.42 (t, J = 8.4 Hz, 1H, Ar-H), 7.25 (t, J = 8.4 Hz, 1H, Ar-H), 6.99 (d, J = 3.2 Hz, 1H, Ar-H), 6.88 (d, J = 8.8 Hz, 1H, Ar-H), 6.84 (dd, J = 6 Hz, 2H, Ar-H), 6.72 (d, J = 5.6 Hz, 1H, Ar-H), 1.64 (m, 2H, $C\mathbf{H}_2CH_2NHSO_2$), 1.4 (m, 2H, $CH_2C\mathbf{H}_2NHSO_2$). ^{13}C NMR (100 MHz, MeOD) δ 161.44 (Ar-C), 158.7 (Ar-C), 157.35 (Ar-C), 147.18 (Ar-C), 146.36 (Ar-C), 130.07 (Ar-C), 129.63 (Ar-C), 128.93 (Ar-C), 128.8 (Ar-C), 128.57 (Ar-C), 125.69 (Ar-C), 119.8 (Ar-C), 115.4 (Ar-C), 115.29 (Ar-C), 114.97 (Ar-C), 111.43 (Ar-C), 106.21 (Ar-C), 42.29 ($CH_2\mathbf{C}H_2NHSO_2$), 41.06 ($\mathbf{C}H_2CH_2NHSO_2$). LC/MS (ESI) 527.9 (M^+).

*5.1.7.11. N-(3-((4-(4-(3-hydroxyphenyl)-2-phenyl-1H-imidazol-5-yl)pyridin-2-yl)amino)propyl)benzenesulfonamide **(11a)***. Yield: 65%. m.p.: 123–125 °C. ^{1}H NMR (400 MHz, MeOD) δ 7.98 (d, J = 7.32 Hz, 2H, Ar-H), 7.83 (q, J = 7.12 Hz, 3H, Ar-H), 7.53 (, J = 7.04 Hz, 3H, Ar-H), 7.46 (q, J = 4.04 Hz, 2H, Ar-H), 7.38 (t, J = 7.2 Hz, 1H, Ar-H), 7.24 (t, J = 8.04 Hz, 1H, Ar-H), 6.99 (t, J = 2.02 Hz, 2H, Ar-H), 6.84 (dd, J = 1.28 Hz, 1H, Ar-H), 6.72 (d, J = 5.52 Hz, 1H, Ar-H), 6.68 (s, 1H, Ar-H), 3.21 (t, J = 6.56 Hz, 2H, $C\mathbf{H}_2CH_2CH_2NHSO_2$), 2.92 (t, J = 6.6 Hz, 2H, $C\mathbf{H}_2CH_2CH_2NHSO_2$), 1.66 (t, J = 6.6 Hz, 2H, $CH_2C\mathbf{H}_2CH_2NHSO_2$). ^{13}C NMR (100 MHz, MeOD) δ 158.78 (Ar-C), 157.35 (Ar-C), 147.19 (Ar-C), 146.28 (Ar-C), 140.26 (Ar-C), 132.26 (Ar-C), 129.6 (Ar-C), 128.88 (Ar-C), 128.58 (Ar-C), 126.58 (Ar-C), 125.71 (Ar-C), 119.85 (Ar-C), 115.47 (Ar-C), 115.04 (Ar-C), 111.11 (Ar-C), 105.96 (Ar-C), 40.3 ($CH_2CH_2\mathbf{C}H_2NHSO_2$), 38.39 ($\mathbf{C}H_2CH_2CH_2NHSO_2$), 28.97 ($CH_2\mathbf{C}H_2CH_2NHSO_2$). LC/MS (ESI) 526.2 ($M^+$).

*5.1.7.12. 4-chloro-N-(3-((4-(4-(3-hydroxyphenyl)-2-phenyl-1H-imidazol-5-yl)pyridin-2-yl)amino)propyl)benzenesulfonamide **(11b)***. Yield: 62%. m.p.: 130–132 °C. ^{1}H NMR (400 MHz, MeOD) δ 7.99 (t, J = 6.92 Hz, 2H, Ar-H), 7.82 (m, 3H, Ar-H), 7.53 (t, J = 2.36 Hz, 1H, Ar-H), 7.51 (t, J = 1.8 Hz, 1H, Ar-H), 7.47 (q, J = 7.68 Hz, 2H, Ar-H), 7.41 (m, 1H, Ar-H), 7.25 (t, J = 7.88 Hz, 1H, Ar-H), 6.99 (t, J = 2.04 Hz, 2H, Ar-H), 6.83 (m, 1H, Ar-H), 6.73 (dd, J = 1.24 Hz, 1H, Ar-H), 6.69 (s, 1H, Ar-H), 3.22 (t, J = 6.64 Hz, 2H, $C\mathbf{H}_2CH_2CH_2NHSO_2$), 2.95 (t, J = 6.72 Hz, 2H, $CH_2CH_2C\mathbf{H}_2NHSO_2$), 1.67 (m, 2H, $CH_2C\mathbf{H}_2CH_2NHSO_2$). ^{13}C NMR (100 MHz, MeOD MeOH) δ 158.81 (Ar-C), 157.37 (Ar-C), 147.17 (Ar-C), 146.31 (Ar-C), 139.17 (Ar-C), 138.35 (Ar-C), 129.63 (Ar-C), 129.04 (Ar-C), 128.78 (Ar-C), 128.55 (Ar-C), 128.29 (Ar-C), 125.69 (Ar-C), 119.82 (Ar-C), 115.45 (Ar-C), 114.99 (Ar-C), 111.06 (Ar-C), 105.94 (Ar-C), 40.28 ($CH_2CH_2\mathbf{C}H_2NHSO_2$), 38.32 ($\mathbf{C}H_2CH_2CH_2NHSO_2$), 28.94 ($CH_2\mathbf{C}H_2CH_2NHSO_2$). LC/MS (ESI) 560.1 ($M^+$).

*5.1.7.13. 4-bromo-N-(3-((4-(4-(3-hydroxyphenyl)-2-phenyl-1H-imidazol-5-yl)pyridin-2-yl)amino)propyl)benzenesulfonamide **(11c)***. Yield: 60%. m.p.: 128–130 °C. HPLC purity 96.3%, ^{1}H NMR (400 MHz, MeOD) δ 8 (d, J = 7.28 Hz, 2H, Ar-H), 7.85 (d, J = 5.44 Hz, 1H, Ar-H), 7.72 (q, J = 8.66 Hz, 4H, Ar-H), 7.49 (t, J = 7.08 Hz, 2H, Ar-H), 7.43 (t, J = 6.28 Hz, 1H, Ar-H), 7.26 (t, J = 7.84 Hz, 1H, Ar-H), 6.99 (t, J = 6.4 Hz, 2H, Ar-H), 6.84 (t, J = 1.48 Hz, 1H, Ar-H), 6.73 (d, J = 5.2 Hz, 1H, Ar-H), 6.68 (s,

1H, Ar-H), 3.23 (t, J = 6.64 Hz, 2H, C**H**$_2$CH$_2$CH$_2$NHSO$_2$), 2.95 (t, J = 6.76 Hz, 2H, CH$_2$CH$_2$C**H**$_2$NHSO$_2$), 1.68 (m, 2H, CH$_2$C**H**$_2$CH$_2$NHSO$_2$). ^{13}C NMR (100 MHz, MeOD) δ 158.95 (Ar-C), 157.4 (Ar-C), 147.14 (Ar-C), 146.54 (Ar-C), 139.73 (Ar-C), 132.06 (Ar-C), 129.67 (Ar-C), 128.75 (Ar-C), 128.37 (Ar-C), 126.67 (Ar-C), 125.67 (Ar-C), 119.77 (Ar-C), 115.42 (Ar-C), 114.97 (Ar-C), 111.02 (Ar-C), 105.91 (Ar-C), 40.28 (CH$_2$CH$_2$**C**H$_2$NHSO$_2$), 38.26 (**C**H$_2$CH$_2$CH$_2$NHSO$_2$), 28.95 (CH$_2$**C**H$_2$CH$_2$NHSO$_2$). $^+$). HRMS calculated for $C_{29}H_{26}BrN_5O_3S$ is 604.5230 found : 605.5318 (M+H).

5.1.7.14. 4-fluoro-N-(3-((4-(4-(3-hydroxyphenyl)-2-phenyl-1H-imidazol-5-yl)pyridin-2-yl)amino)propyl)benzenesulfonamide ***(11d)***. Yield: 75%. m.p.: 147–149 °C. HPLC purity 96.5%,^{1}H NMR (400 MHz, MeOD) δ 7.98 (d, J = 7.2 Hz, 2H, Ar-H), 7.88 (m, 2H, Ar-H), 7.83 (d, J = 5.6 Hz, 1H, Ar-H), 7.46 (t, J = 7.2 Hz, 2H, Ar-H), 7.4 (t, J = 7.2 Hz, 1H, Ar-H), 7.26 (q, J = 2 Hz, 3H, Ar-H), 6.99 (d, J = 8.4 Hz, 2H, Ar-H), 6.83 (dd, J = 1.6 Hz, 1H, Ar-H), 6.71 (d, J = 5.2 Hz, 1H, Ar-H), 6.68 (s, 1H, Ar-H), 3.22 (t, J = 6.8 Hz, 2H, C**H**$_2$CH$_2$CH$_2$NHSO$_2$), 2.93 (t, J = 6.4 Hz, 2H, CH$_2$CH$_2$C**H**$_2$NHSO$_2$), 1.67 (m, 2H, CH$_2$C**H**$_2$CH$_2$NHSO$_2$). ^{13}C NMR (100 MHz, MeOD) δ 166.16 (Ar-C), 163.66 (Ar-C), 158.95 (Ar-C), 157.54 (Ar-C), 136.67 (Ar-C), 129.65 (Ar-C), 129.46 (Ar-C), 128.78 (Ar-C), 128.56 (Ar-C), 125.69 (Ar-C), 119.8 (Ar-C), 115.96 (Ar-C), 115.44 (Ar-C), 114.97 (Ar-C), 111.07 (Ar-C), 105.96 (Ar-C), 40.28 (CH$_2$CH$_2$**C**H$_2$NHSO$_2$), 38.33 (**C**H$_2$CH$_2$CH$_2$NHSO$_2$), 29.37 (CH$_2$**C**H$_2$CH$_2$NHSO$_2$). 19F NMR (400 MHz, DMSO-d_6) −107.24 (d, 1F, J = 56 Hz). LC/MS (ESI) 544.1 (M+1) $^+$.

5.1.7.15. 3-chloro-N-(3-((4-(4-(3-hydroxyphenyl)-2-phenyl-1H-imidazol-5-yl)pyridin-2-yl)amino)propyl)benzenesulfonamide ***(11e)***. Yield: 70%. m.p.: 142–144 °C. ^{1}H NMR (400 MHz, MeOD) δ 7.99 (d, J = 1.36 Hz, 1H, Ar-H), 7.98 (s, 1H, Ar-H), 7.84 (m, 2H, Ar-H), 7.76 (dt, J = 1.04 Hz, 1H, Ar-H), 7.57 (m, 1H, Ar-H), 7.48 (m, 3H, Ar-H), 7.41 (m, 1H, Ar-H), 7.25 (t, J = 7.84 Hz, 1H, Ar-H), 6.98 (m, 2H, Ar-H), 6.84 (dd, J = 1.72 Hz, 1H, Ar-H), 6.72 (dd, J = 1.12 Hz, 1H, Ar-H), 6.68 (s, 1H, Ar-H), 3.23 (t, J = 6.68 Hz, 2H, C**H**$_2$CH$_2$CH$_2$NHSO$_2$), 2.95 (t, J = 6.76 Hz, 2H, CH$_2$CH$_2$C**H**$_2$NHSO$_2$), 1.68 (m, 2H, CH$_2$C**H**$_2$CH$_2$NHSO$_2$). ^{13}C NMR (100 MHz, MeOD) δ 158.85 (Ar-C), 157.36 (Ar-C), 147.16 (Ar-C), 146.36 (Ar-C), 142.35 (Ar-C), 134.77 (Ar-C), 132.17 (Ar-C), 130.5 (Ar-C), 129.56 (Ar-C), 128.55 (Ar-C), 126.46 (Ar-C), 125.68 (Ar-C), 124.95 (Ar-C), 119.81 (Ar-C), 115.44 (Ar-C), 111.07 (Ar-C), 105.96 (Ar-C), 40.3 (CH$_2$CH$_2$**C**H$_2$NHSO$_2$), 38.32 (**C**H$_2$CH$_2$CH$_2$NHSO$_2$), 28.99 (CH$_2$**C**H$_2$CH$_2$NHSO$_2$). LC/MS (ESI) 560.2 (M$^+$).

5.1.7.16. 2,6-dichloro-N-(3-((4-(4-(3-hydroxyphenyl)-2-phenyl-1H-imidazol-5-yl)pyridin-2-yl)amino)propyl)benzenesulfonamide ***(11f)***. Yield: 75%. m.p.: 138–140 °C. ^{1}H NMR (400 MHz, MeOD) δ 7.99 (d, J = 6.48 Hz, 2H, Ar-H), 7.83 (d, J = 4.28 Hz, 1H, Ar-H), 7.48 (d, J = 6.88 Hz, 4H, Ar-H), 7.39 (dd, J = 6.56 Hz, 2H, Ar-H), 7.24 (d, J = 7.2 Hz, 1H, Ar-H), 6.99 (d, J = 8.08 Hz, 2H, Ar-H), 6.84 (d, J = 6.48 Hz, 1H, Ar-H), 6.7 (m, 2H, Ar-H), 3.23 (s, 2H, C**H**$_2$CH$_2$CH$_2$NHSO$_2$), 3.07 (s, 2H, CH$_2$CH$_2$C**H**$_2$NHSO$_2$), 1.69 (s, 2H, CH$_2$C**H**$_2$CH$_2$NHSO$_2$). ^{13}C NMR (100 MHz, MeOD) δ 158.84 (Ar-C), 157.36 (Ar-C), 147.15 (Ar-C), 146.41 (Ar-C), 135.76 (Ar-C), 134.51 (Ar-C), 131.32 (Ar-C), 129.59 (Ar-C), 128.79 (Ar-C), 125.69 (Ar-C), 119.82 (Ar-C), 115.44 (Ar-C), 115 (Ar-C), 111.09 (Ar-C), 105.99 (Ar-C), 40.06 (CH$_2$CH$_2$**C**H$_2$NHSO$_2$), 38.28 (**C**H$_2$CH$_2$CH$_2$NHSO$_2$), 29.4 (CH$_2$**C**H$_2$CH$_2$NHSO$_2$). LC/MS (ESI) 594.2 (M$^+$).

5.1.7.17. 3-fluoro-N-(3-((4-(4-(3-hydroxyphenyl)-2-phenyl-1H-imidazol-5-yl)pyridin-2-yl)amino)propyl)benzenesulfonamide ***(11g)***. Yield: 60%. m.p.: 140–142 °C. ^{1}H NMR (400 MHz, MeOD) δ 7.99 (d, J = 6.88 Hz, 2H, Ar-H), 7.83 (d, J = 4.8 Hz, 1H, Ar-H), 7.67 (d, J = 7.24 Hz, 1H, Ar-H), 7.56 (m, 2H, Ar-H), 7.43 (m, 3H, Ar-H), 7.32 (dt, J = 6.96 Hz, 2H, Ar-H), 6.98 (s, 2H, Ar-H), 6.84 (d, J = 7.28 Hz, 1H, Ar-H), 6.7 (m, 2H, Ar-H), 3.23 (s, 2H, C**H**$_2$CH$_2$CH$_2$NHSO$_2$), 2.96 (s, 2H, CH$_2$CH$_2$C**H**$_2$NHSO$_2$), 1.68 (t, J = 5.68 Hz, 2H, CH$_2$C**H**$_2$CH$_2$NHSO$_2$). ^{13}C NMR (100 MHz, MeOD) δ 163.7 (Ar-C), 161.22 (Ar-C), 158.8 (Ar-C), 157.35 (Ar-C), 147.18 (Ar-C), 142.64 (Ar-C), 131.03 (Ar-C), 130.95 (Ar-C), 129.59 (Ar-C), 128.56 (Ar-C), 125.7 (Ar-C), 122.59 (Ar-C), 119.07 (Ar-C), 115.46 (Ar-C), 113.78 (Ar-C), 111.1 (Ar-C), 105.97 (Ar-C), 40.32 (CH$_2$CH$_2$**C**H$_2$NHSO$_2$), 38.35 (**C**H$_2$CH$_2$CH$_2$NHSO$_2$), 28.99 (CH$_2$**C**H$_2$CH$_2$NHSO$_2$). LC/MS (ESI) 544.2 (M+1) $^+$.

5.1.7.18. N-(3-((4-(4-(3-hydroxyphenyl)-2-phenyl-1H-imidazol-5-yl)pyridin-2-yl)amino)propyl)-4-(trifluoromethyl)benzenesulfonamide ***(11h)***. Yield: 70%. m.p.: 118–120 °C. ^{1}H NMR (400 MHz, MeOD) δ 8.03 (d, J = 8.2 Hz, 2H, Ar-H), 8 (d, J = 7.2 Hz, 2H, Ar-H), 7.87 (s, 1H, Ar-H), 7.83 (t, J = 4.36 Hz, 2H, Ar-H), 7.47 (t, J = 8 Hz, 2H, Ar-H), 7.41 (t, J = 7.2 Hz, 1H, Ar-H), 7.25 (t, J = 7.8 Hz, 1H, Ar-H), 7 (d, J = 8 Hz, 2H, Ar-H), 6.84 (dd, J = 1.72 Hz, 1H, Ar-H), 6.72 (t, J = 4.2 Hz, 2H, Ar-H), 3.24 (t, J = 6.64 Hz, 2H, C**H**$_2$CH$_2$CH$_2$NHSO$_2$), 2.98 (t, J = 6.72 Hz, 2H, CH$_2$CH$_2$C**H**$_2$NHSO$_2$), 1.69 (m, 2H, CH$_2$C**H**$_2$CH$_2$NHSO$_2$). ^{13}C NMR (100 MHz, MeOD) δ 158.7665 (Ar-C), 157.3769 (Ar-C), 147.1943 (Ar-C), 144.4041 (Ar-C), 133.6514 (Ar-C), 129.6259 (Ar-C), 127.3952 (Ar-C), 126.0172 (Ar-C), 125.9802 (Ar-C), 124.8846 (Ar-C), 122.1808 (Ar-C), 119.814 (Ar-C), 115.4464 (Ar-C), 111.0724 (Ar-C), 105.9958 (Ar-C), 40.3301 (CH$_2$CH$_2$**C**H$_2$NHSO$_2$), 38.3261 (**C**H$_2$CH$_2$CH$_2$NHSO$_2$), 29.0156 (CH$_2$**C**H$_2$CH$_2$NHSO$_2$). LC/MS (ESI) 594.1 (M+1) $^+$.

5.1.7.19. N-(3-((4-(4-(3-hydroxyphenyl)-2-phenyl-1H-imidazol-5-yl)pyridin-2-yl)amino)propyl)-4-methoxybenzenesulfonamide ***(11i)***. Yield: 70%. m.p.: 120–122 °C. ^{1}H NMR (400 MHz, MeOD) δ 8 (d, J = 7.24 Hz, 2H, Ar-H), 7.84 (d, J = 5.16 Hz, 1H, Ar-H), 7.77 (d, J = 8.6 Hz, 2H, Ar-H), 7.49 (t, J = 7.04 Hz, 2H, Ar-H), 7.43 (d, J = 6.92 Hz, 1H, Ar-H), 7.26 (t, J = 7.68 Hz, 1H, Ar-H), 7.01 (t, J = 8.8 Hz, 4H, Ar-H), 6.84 (d, J = 8.4 Hz, 1H, Ar-H), 6.73 (d, J = 5 Hz, 1H, Ar-H), 6.69 (s, 1H, Ar-H), 2.83 (s, 3H, OC**H**$_3$), 3.23 (t, J = 6.04 Hz, 2H, C**H**$_2$CH$_2$CH$_2$NHSO$_2$), 2.91 (t, J = 6.4 Hz, 2H, CH$_2$CH$_2$C**H**$_2$NHSO$_2$), 1.67 (t, J = 6.4 Hz, 2H, CH$_2$C**H**$_2$CH$_2$NHSO$_2$). ^{13}C NMR (100 MHz, MeOD) δ 162.9251 (Ar-C), 158.8438 (Ar-C), 147.1582 (Ar-C), 131.7538 (Ar-C), 129.5501 (Ar-C), 128.904 (Ar-C), 128.5467 (Ar-C), 125.6733 (Ar-C), 119.7921 (Ar-C), 115.4281 (Ar-C), 114.9691 (Ar-C), 110.9773 (Ar-C), 105.9006 (Ar-C), 54.7721 (O**C**H$_3$), 40.2178 (CH$_2$CH$_2$**C**H$_2$NHSO$_2$), 38.3466 (**C**H$_2$CH$_2$CH$_2$NHSO$_2$), 28.9007 (CH$_2$**C**H$_2$CH$_2$NHSO$_2$). LC/MS (ESI) 556.1 (M+1) $^+$.

5.1.7.20. 4-hydroxy-N-(3-((4-(4-(3-hydroxyphenyl)-2-phenyl-1H-imidazol-5-yl)pyridin-2-yl)amino)propyl)benzenesulfonamide ***(11j)***. Yield: 60%. m.p.: 130–132 °C. ^{1}H NMR (400 MHz, MeOD) δ 7.97 (d, J = 7.2 Hz, 2H, Ar-H), 7.8 (d, J = 5.6 Hz, 1H, Ar-H), 7.68 (d, J = 8.4 Hz, 2H, Ar-H), 7.44 (t, J = 4.6 Hz, 2H, Ar-H), 7.38 (t, J = 7.2 Hz, 1H, Ar-H), 7.24 (t, J = 8.4 Hz, 1H, Ar-H), 6.99 (d, J = 6.4 Hz, 2H, Ar-H), 6.89 (d, J = 8.8 Hz, 2H, Ar-H), 6.84 (dd, J = 1.2 Hz, 1H, Ar-H), 6.71 (t, J = 2.8 Hz, 2H, Ar-H), 3.21 (t, J = 6.4 Hz, 2H, C**H**$_2$CH$_2$CH$_2$NHSO$_2$), 2.89 (t, J = 6.4 Hz, 2H, CH$_2$CH$_2$C**H**$_2$NHSO$_2$), 1.66 (t, J = 6.4 Hz, 2H, CH$_2$C**H**$_2$CH$_2$NHSO$_2$). ^{13}C NMR (100 MHz, MeOD) δ 161.39 (Ar-C), 158.44 (Ar-C), 157.33 (Ar-C), 147.27 (Ar-C), 145.63 (Ar-C), 130.11 (Ar-C), 129.66 (Ar-C), 128.97 (Ar-C), 128.59 (Ar-C), 125.73 (Ar-C), 119.89 (Ar-C), 115.47 (Ar-C), 115.35 (Ar-C), 111.08 (Ar-C), 106.05 (Ar-C), 40.24 (CH$_2$CH$_2$**C**H$_2$NHSO$_2$), 38.47 (**C**H$_2$CH$_2$CH$_2$NHSO$_2$), 28.84 (CH$_2$**C**H$_2$CH$_2$NHSO$_2$). LC/MS (ESI) 542.1 (M+1) $^+$.

5.2. Pharmacological screening

5.2.1. In vitro P38α kinase assay

Thermo Fisher Scientific, SelectScreen Kinase Profiling Services was used for screening of the target compounds in single point concentrations mode, and 5-points titration mode for IC_{50} determination.

Assay protocol: as reported on Thermo Fisher Scientific website using 100 μM concentration of ATP.

5.2.2. Inflammatory cytokines production assay

5.2.2.1. Cell culture and treatment. RAW 264.7 macrophages were obtained from the Korean Cell Line Bank. Mouse peritoneal macrophage cells were obtained 4 days after the intraperitoneal injection of 2 mL of thioglycollate to the 10-week-old C57BL/6 male mice and isolated.

The cells were treated with the tested compounds and then stimulated with lipopolysaccharide (LPS) (100 ng/mL) for the incubated time.

5.2.2.2. PGE_2 and cytokine production assay. After 24 h incubation, the supernatant was collected and PGE_2, IL-1β, TNF-α, and IL-6 levels in cell culture media were quantified by PGE_2 (Enzo Life Sciences, Inc., Farmingdale, NY, USA), IL-1β (R&D Systems, MN, USA), and TNF-α and IL-6 (BD Bio-science, Sand Diego, CA, USA) enzyme immunoassay (EIA) kits according to the manufacturer's instructions. N-[2-(Cyclohexyloxy)-4-nitrophenyl]methanesulfonamide (NS-398), a selective cyclooxygenase-2 (COX-2) inhibitor, was purchased from Sigma Aldrich (St. Louis, MO, USA) and used as a positive control for blocking PGE_2 production.[50]

5.2.3. Nitric oxide assay

After 24 h incubation with the tested compound and LPS, the supernatant was collected and nitrite levels in culture media were detected using Griess reaction and presumed to reflect NO levels. LN6 -(1-Iminoethyl)lysine dihydrochloride (L-NIL) was used as a positive control for blocking NO production.

5.3. Molecular modeling studies

5.3.1. Molecular docking study

The X-ray crystal structure of P38α in complex with **SB203580** (PDB ID: 3GCP) was downloaded from the protein data bank (www.rcsb.org) in PDB format. The 2D structure of the target compounds were assembled using ChemDraw software. Molecular Operating Environment (MOE) software was used for the molecular docking operation of the target compounds **8a-i**, **9a-i**, **10a-j**, and **11a-j** with P38α kinase enzyme domain (PDB ID: 3GCP). The protein structure was prepared for the molecular docking procedure by applying 3D protonation of both enzyme amino acids and the native ligand (SB203580). In addition, water of crystallization was removed from the kinase domain. The active site was isolated. The docking simulation of native ligands (SB203580) with the active site of P38α kinase (PDB ID: 3GCP) was investigated in order to validate the docking protocol. Both 3D protonation and energy minimization were performed for the target compounds using MOE software.

5.3.2. Molecular dynamics simulations

The molecular dynamics (MD) simulations study was carried out for the obtained docked protein complex of the native ligand **SB203580** and compound **11d**, using standard default parameter setting in the MOE 2014 software in order to examine the conformational stability of their docked complexes in the active site of the corresponding kinase (PDB ID: 3GCP).

MOE implemented four algorithms, the Nos_e-Poincar_e-Andesen (NPA), the Nos_e-Hoover-Andersen (NHA), Berendsen velocity/position (BER) and Nanoscale Molecular Dynamics (NAMD). In this study, MD calculations were performed by using NPA, the most precise algorithm for long-time simulations.[51] The system optimization was obtained by energy minimization, applying MMFF94x force field, water as a solvent, six margins and delete far existing solvent with distance greater than 4 Å.

The MD simulation protocol was run for 600 ns at 300 K temperature, the potential energy (kcal/mole) was recorded at intervals of 0.5 ns.

Also, the root mean square deviation (RMSD) values were observed during the whole MD simulation process in order to determine the stability of the ligand-receptor complex during the MD simulation.

Declaration of Competing Interest

The authors declare that they have no known competing financial interests or personal relationships that could have appeared to influence the work reported in this paper.

Acknowledgements

This work was supported by Korea Institute of Science and Technology (KIST), and KIST Project (2E29340).

Declaration of Competing Interest

The authors declare that they have no known competing financial interests or personal relationships that could have appeared to influence the work reported in this paper.

Appendix A. Supplementary material

Supplementary data to this article can be found online at https://doi.org/10.1016/j.bmc.2020.115969.

References

1 Tong L, et al. A highly specific inhibitor of human p38 MAP kinase binds in the ATP pocket. *Nat Struct Biol.* 1997;4(4):311–316.
2 Peti W, Page R. Molecular basis of MAP kinase regulation. *Protein Sci.* 2013;22(12):1698–1710.
3 Schett G, et al. How antirheumatic drugs protect joints from damage in rheumatoid arthritis. *Arthritis Rheumatism: Off J Am College Rheumatol.* 2008;58(10):2936–2948.
4 Du Y, et al. MKP-1 reduces Aβ generation and alleviates cognitive impairments in Alzheimer's disease models. *Signal Transduct Target Ther.* 2019;4(1):1–12.
5 Laufer SA, et al. Design, synthesis, and biological evaluation of novel Tri-and tetrasubstituted imidazoles as highly potent and specific ATP-mimetic inhibitors of p38 MAP kinase: Focus on optimized interactions with the enzyme's surface-exposed front region. *J Med Chem.* 2008;51(14):4122–4149.
6 Dhillon AS, et al. MAP kinase signalling pathways in cancer. *Oncogene.* 2007;26(22):3279–3290.
7 Nebreda AR, Porras A. p38 MAP kinases: beyond the stress response. *Trends Biochem Sci.* 2000;25(6):257–260.
8 Enslen H, Brancho DM, Davis RJ. Molecular determinants that mediate selective activation of p38 MAP kinase isoforms. *EMBO J.* 2000;19(6):1301–1311.
9 Cuenda A, Rousseau S. *p38 MAP-kinases pathway regulation, function and role in human diseases.* Biochimica et Biophysica Acta (BBA)-Molecular. *Cell Res.* 2007;1773(8):1358–1375.
10 El-Gamal MI, et al. Discovery of a potent p38α/MAPK14 kinase inhibitor: synthesis, in vitro/in vivo biological evaluation, and docking studies. *Eur J Med Chem.* 2019;183:111684.
11 Schieven GL. The biology of p38 kinase: a central role in inflammation. *Curr Top Med Chem.* 2005;5(10):921–928.
12 Westra J, et al. Chemokine production and E-selectin expression in activated endothelial cells are inhibited by p38 MAPK (mitogen activated protein kinase) inhibitor RWJ 67657. *Int Immunopharmacol.* 2005;5(7–8):1259–1269.
13 Takami M, et al. Phosphodiesterase inhibitors stimulate osteoclast formation via TRANCE/RANKL expression in osteoblasts: possible involvement of ERK and p38 MAPK pathways. *FEBS Lett.* 2005;579(3):832–838.
14 Berghe WV, et al. Signal transduction by tumor necrosis factor and gene regulation of the inflammatory cytokine interleukin-6. *Biochem Pharmacol.* 2000;60(8):1185–1195.
15 Guijas C, et al. Simultaneous activation of p38 and JNK by arachidonic acid stimulates the cytosolic phospholipase A2-dependent synthesis of lipid droplets in human monocytes. *J Lipid Res.* 2012;53(11):2343–2354.
16 Ayala JM, et al. Serum-induced monocyte differentiation and monocyte chemotaxis are regulated by the p38 MAP kinase signal transduction pathway. *J Leukoc Biol.* 2000;67(6):869–875.
17 Tamhane M, et al. Comparative renal excretion of VX-702, a novel p38 MAPK inhibitor, and methotrexate in the perfused rat kidney model. *Drug Dev Ind Pharm.* 2010;36(3):315–322.
18 Zhu D, et al. Synthesis and p38 inhibitory activity of some novel substituted N, N′-diarylurea derivatives. *Molecules.* 2016;21(5):677.
19 Azevedo R, et al. X-ray structure of p38α bound to TAK-715: comparison with three classic inhibitors. *Acta Crystallogr D Biol Crystallogr.* 2012;68(8):1041–1050.
20 Gilani RA, et al. UM-164: a potent c-Src/p38 kinase inhibitor with in vivo activity against triple-negative breast cancer. *Clin Cancer Res.* 2016;22(20):5087–5096.

21 Burnette BL, et al. SD0006: a potent, selective and orally available inhibitor of p38 kinase. *Pharmacology*. 2009;84(1):42–60.
22 Fu Y, et al. The p38 MAPK inhibitor, PD169316, inhibits transforming growth factor β-induced Smad signaling in human ovarian cancer cells. *Biochem Biophys Res Commun*. 2003;310(2):391–397.
23 Cohen SB, et al. Evaluation of the efficacy and safety of pamapimod, a p38 MAP kinase inhibitor, in a double-blind, methotrexate-controlled study of patients with active rheumatoid arthritis. *Arthritis Rheumat: Off J Am College Rheumatol*. 2009;60 (2):335–344.
24 Mihara K, et al. A potent and selective p38 inhibitor protects against bone damage in murine collagen-induced arthritis: a comparison with neutralization of mouse TNFα. *Br J Pharmacol*. 2008;154(1):153–164.
25 Newby LK, et al. Losmapimod, a novel p38 mitogen-activated protein kinase inhibitor, in non-ST-segment elevation myocardial infarction: a randomised phase 2 trial. *The Lancet*. 2014;384(9949):1187–1195.
26 Moon S-H, Choi S-W, Kim SH. In vitro anti-osteoclastogenic activity of p38 inhibitor doramapimod via inhibiting migration of pre-osteoclasts and NFATc1 activity. *J Pharmacol Sci*. 2015;129(3):135–142.
27 Kang JS, et al. DMB1285 [cyclopropyl-{4-[4-(4-fluorophenyl)-2-piperidin-4-yl-thiazol-5-yl] pyrimidin-2-yl} amine] suppresses tumor necrosis factor-α production by blocking p38 mitogen-activated protein kinase/mitogen-activated protein kinase-activated protein kinase 2 signaling pathway. *J Pharmacol Exp Ther*. 2010.
28 Liu C, et al. Discovery of 4-(5-(cyclopropylcarbamoyl)-2-methylphenylamino)-5-methyl-N-propylpyrrolo [1, 2-f][1, 2, 4] triazine-6-carboxamide (BMS-582949), a clinical p38α MAP kinase inhibitor for the treatment of inflammatory diseases. *J Med Chem*. 2010;53(18):6629–6639.
29 Dominguez C, Powers DA, Tamayo N. p38 MAP kinase inhibitors: many are made, but few are chosen. *Curr Opin Drug Discov Devel*. 2005;8(4):421–430.
30 Ali EM, et al. Design, synthesis, and biological evaluation of novel imidazole derivatives possessing terminal sulphonamides as potential BRAFV600E inhibitors. *Bioorg Chem*. 2020:104508.
31 Yang H, et al. RG7204 (PLX4032), a selective BRAFV600E inhibitor, displays potent antitumor activity in preclinical melanoma models. *Cancer Res*. 2010;70(13): 5518–5527.
32 Ono K, Han J. The p38 signal transduction pathway activation and function. *Cell Signal*. 2000;12(1):1–13.
33 Wagner EF, Nebreda ÁR. Signal integration by JNK and p38 MAPK pathways in cancer development. *Nat Rev Cancer*. 2009;9(8):537–549.
34 Needleman SB, Wunsch CD. A general method applicable to the search for similarities in the amino acid sequence of two proteins. *J Mol Biol*. 1970;48(3): 443–453.
35 Simard JR, et al. Development of a fluorescent-tagged kinase assay system for the detection and characterization of allosteric kinase inhibitors. *J Am Chem Soc*. 2009; 131(37):13286–13296.
36 Manthey CL, et al. SB202190, a selective inhibitor of p38 mitogen-activated protein kinase, is a powerful regulator of LPS-induced mRNAs in monocytes. *J Leukoc Biol*. 1998;64(3):409–417.
37 Fijen J, et al. Suppression of the clinical and cytokine response to endotoxin by RWJ-67657, a p38 mitogen-activated protein-kinase inhibitor, in healthy human volunteers. *Clin Exp Immunol*. 2001;124(1):16–20.
38 Badger A, et al. Differential effects of SB 242235, a selective p38 mitogen-activated protein kinase inhibitor, on IL-1 treated bovine and human cartilage/chondrocyte cultures. *Osteoarthritis Cartilage*. 2000;8(6):434–443.
39 Carta A, et al. Novel substituted quinoxaline 1, 4-dioxides with in vitro antimycobacterial and anticandida activity. *Eur J Med Chem*. 2002;37(5):355–366.
40 McClure KF, et al. Theoretical and experimental design of atypical kinase inhibitors: application to p38 MAP kinase. *J Med Chem*. 2005;48(18):5728–5737.
41 Tariq S, Alam O, Amir M. Synthesis, anti-inflammatory, p38α MAP kinase inhibitory activities and molecular docking studies of quinoxaline derivatives containing triazole moiety. *Bioorg Chem*. 2018;76:343–358.
42 Somakala K, Tariq S, Amir M. Synthesis, evaluation and docking of novel pyrazolo pyrimidines as potent p38α MAP kinase inhibitors with improved anti-inflammatory, ulcerogenic and TNF-α inhibitory properties. *Bioorg Chem*. 2019;87:550–559.
43 Liu C, et al. Benzothiazole based inhibitors of p38α MAP kinase. *Bioorg Med Chem Lett*. 2008;18(6):1874–1879.
44 Heider F, et al. Pyridinylimidazoles as dual glycogen synthase kinase 3β/p38α mitogen-activated protein kinase inhibitors. *Eur J Med Chem*. 2019;175:309–329.
45 Jacobs AT, Ignarro LJ. Lipopolysaccharide-induced expression of interferon-β mediates the timing of inducible nitric-oxide synthase induction in RAW 264.7 macrophages. *J Biol Chem*. 2001;276(51):47950–47957.
46 Amano F, Noda T. Improved detection of nitric oxide radical (NO•) production in an activated macrophage culture with a radical scavenger, car□ y PTIO, and Griess reagent. *FEBS Lett*. 1995;368(3):425–428.
47 Moore WM, et al. L-N6-(1-iminoethyl) lysine: a selective inhibitor of inducible nitric oxide synthase. *J Med Chem*. 1994;37(23):3886–3888.
48 Aroonrerk N, Suksamrarn A, Kirtikara K. A sensitive direct ELISA for detection of prostaglandin E2. *J Immunoassay Immunochem*. 2007;28(4):319–330.
49 Futaki N, et al. NS-398, a new anti-inflammatory agent, selectively inhibits prostaglandin G/H synthase/cyclooxygenase (COX-2) activity in vitro. *Prostaglandins*. 1994;47(1):55–59.
50 Han H-S, et al. Cirsimarin, a flavone glucoside from the aerial part of Cirsium japonicum var. ussuriense (Regel) Kitam. ex Ohwi, suppresses the JAK/STAT and IRF-3 signaling pathway in LPS-stimulated RAW 264.7 macrophages. *Chem Biol Interact*. 2018;293:38–47.
51 Sturgeon JB, Laird BB. Symplectic algorithm for constant-pressure molecular dynamics using a Nosé-Poincaré thermostat. *J Chem Phys*. 2000;112(8):3474–3482.